**Huang, Y. L. and Niehrs, C.** (2014). Polarized Wnt signaling regulates ectodermal cell fate in Xenopus. *Dev. Cell* **29**, 250-257.
**Janda, C. Y., Waghray, D., Levin, A. M., Thomas, C. and Garcia, K. C.** (2012). Structural basis of Wnt recognition by Frizzled. *Science* **337**, 59-64.
**Kikuchi, A., Yamamoto, H., Sato, A. and Matsumoto, S.** (2011). New insights into the mechanism of Wnt signaling pathway activation. *Int. Rev. Cell Mol. Biol.* **291**, 21-71.
**Kim, G. H., Her, J. H. and Han, J. K.** (2008). Ryk cooperates with Frizzled 7 to promote Wnt11-mediated endocytosis and is essential for Xenopus laevis convergent extension movements. *J. Cell Biol.* **182**, 1073-1082.
**Kimura, M., Kose, S., Okumura, N., Imai, K., Furuta, M., Sakiyama, N., Tomii, K., Horton, P., Takao, T. and Imamoto, N.** (2013). Identification of cargo proteins specific for the nucleocytoplasmic transport carrier transportin by combination of an in vitro transport system and stable isotope labeling by amino acids in cell culture (SILAC)-based quantitative proteomics. *Mol. Cell. Proteomics* **12**, 145-157.
**Komekado, H., Yamamoto, H., Chiba, T. and Kikuchi, A.** (2007). Glycosylation and palmitoylation of Wnt-3a are coupled to produce an active form of Wnt-3a. *Genes Cells* **12**, 521-534.
**Kurayoshi, M., Yamamoto, H., Izumi, S. and Kikuchi, A.** (2007). Post-translational palmitoylation and glycosylation of Wnt-5a are necessary for its signalling. *Biochem. J.* **402**, 515-523.
**Li, F. F., Zhang, T., Bai, Y. Z., Yuan, Z. W. and Wang, W. L.** (2011). Spatiotemporal expression of Wnt5a during the development of the hindgut and anorectum in human embryos. *Int. J. Colorectal Dis.* **26**, 983-988.
**Logan, C. Y. and Nusse, R.** (2004). The Wnt signaling pathway in development and disease. *Annu. Rev. Cell Dev. Biol.* **20**, 781-810.
**Lu, W., Yamamoto, V., Ortega, B. and Baltimore, D.** (2004). Mammalian Ryk is a Wnt coreceptor required for stimulation of neurite outgrowth. *Cell* **119**, 97-108.
**Martín-Belmonte, F., Yu, W., Rodríguez-Fraticelli, A. E., Ewald, A. J., Werb, Z., Alonso, M. A. and Mostov, K.** (2008). Cell-polarity dynamics controls the mechanism of lumen formation in epithelial morphogenesis. *Curr. Biol.* **18**, 507-513.
**Matsumoto, S., Fumoto, K., Okamoto, T., Kaibuchi, K. and Kikuchi, A.** (2010). Binding of APC and dishevelled mediates Wnt5a-regulated focal adhesion dynamics in migrating cells. *EMBO J.* **29**, 1192-1204.
**Myllymäki, S. M., Teräväinen, T. P. and Manninen, A.** (2011). Two distinct integrin-mediated mechanisms contribute to apical lumen formation in epithelial cells. *PLoS ONE* **6**, e19453.
**Nishita, M., Enomoto, M., Yamagata, K. and Minami, Y.** (2010). Cell/tissue-tropic functions of Wnt5a signaling in normal and cancer cells. *Trends Cell Biol.* **20**, 346-354.
**O'Brien, L. E., Jou, T. S., Pollack, A. L., Zhang, Q., Hansen, S. H., Yurchenco, P. and Mostov, K. E.** (2001). Rac1 orientates epithelial apical polarity through effects on basolateral laminin assembly. *Nat. Cell Biol.* **3**, 831-838.
**Polakis, P.** (2007). The many ways of Wnt in cancer. *Curr. Opin. Genet. Dev.* **17**, 45-51.
**Port, F. and Basler, K.** (2010). Wnt trafficking: new insights into Wnt maturation, secretion and spreading. *Traffic* **11**, 1265-1271.
**Rademacher, T. W., Parekh, R. B. and Dwek, R. A.** (1988). Glycobiology. *Annu. Rev. Biochem.* **57**, 785-838.
**Sakane, H., Yamamoto, H., Matsumoto, S., Sato, A. and Kikuchi, A.** (2012). Localization of glypican-4 in different membrane microdomains is involved in the regulation of Wnt signaling. *J. Cell Sci.* **125**, 449-460.
**Sato, A., Yamamoto, H., Sakane, H., Koyama, H. and Kikuchi, A.** (2010). Wnt5a regulates distinct signalling pathways by binding to Frizzled2. *EMBO J.* **29**, 41-54.
**Schulte, G. and Bryja, V.** (2007). The Frizzled family of unconventional G-protein-coupled receptors. *Trends Pharmacol. Sci.* **28**, 518-525.
**Simmen, T., Höning, S., Icking, A., Tikkanen, R. and Hunziker, W.** (2002). AP-4 binds basolateral signals and participates in basolateral sorting in epithelial MDCK cells. *Nat. Cell Biol.* **4**, 154-159.
**Spiro, R. G.** (2002). Protein glycosylation: nature, distribution, enzymatic formation, and disease implications of glycopeptide bonds. *Glycobiology* **12**, 43R-56R.
**Strutt, D.** (2003). Frizzled signalling and cell polarisation in Drosophila and vertebrates. *Development* **130**, 4501-4513.
**Takada, R., Satomi, Y., Kurata, T., Ueno, N., Norioka, S., Kondoh, H., Takao, T. and Takada, S.** (2006). Monounsaturated fatty acid modification of Wnt protein: its role in Wnt secretion. *Dev. Cell* **11**, 791-801.
**Uysal-Onganer, P. and Kypta, R. M.** (2012). Wnt11 in 2011 – the regulation and function of a non-canonical Wnt. *Acta Physiol. (Oxf.)* **204**, 52-64.
**Vagin, O., Kraut, J. A. and Sachs, G.** (2009). Role of N-glycosylation in trafficking of apical membrane proteins in epithelia. *Am. J. Physiol.* **296**, F459-F469.
**Willert, K., Brown, J. D., Danenberg, E., Duncan, A. W., Weissman, I. L., Reya, T., Yates, J. R., III and Nusse, R.** (2003). Wnt proteins are lipid-modified and can act as stem cell growth factors. *Nature* **423**, 448-452.
**Wu, J., Klein, T. J. and Mlodzik, M.** (2004). Subcellular localization of frizzled receptors, mediated by their cytoplasmic tails, regulates signaling pathway specificity. *PLoS Biol.* **2**, e158.
**Yagi, S., Matsuda, M. and Kiyokawa, E.** (2012). Suppression of Rac1 activity at the apical membrane of MDCK cells is essential for cyst structure maintenance. *EMBO Rep.* **13**, 237-243.
**Yamada, M., Udagawa, J., Matsumoto, A., Hashimoto, R., Hatta, T., Nishita, M., Minami, Y. and Otani, H.** (2010). Ror2 is required for midgut elongation during mouse development. *Dev. Dyn.* **239**, 941-953.
**Yamamoto, H., Komekado, H. and Kikuchi, A.** (2006). Caveolin is necessary for Wnt-3a-dependent internalization of LRP6 and accumulation of β-catenin. *Dev. Cell* **11**, 213-223.
**Yamamoto, H., Awada, C., Hanaki, H., Sakane, H., Tsujimoto, I., Takahashi, Y., Takao, T. and Kikuchi, A.** (2013). The apical and basolateral secretion of Wnt11 and Wnt3a in polarized epithelial cells is regulated by different mechanisms. *J. Cell Sci.* **126**, 2931-2943.
**Yamanaka, H. and Nishida, E.** (2007). Wnt11 stimulation induces polarized accumulation of Dishevelled at apical adherens junctions through Frizzled7. *Genes Cells* **12**, 961-967.
**Yeaman, C., Grindstaff, K. K. and Nelson, W. J.** (1999). New perspectives on mechanisms involved in generating epithelial cell polarity. *Physiol. Rev.* **79**, 73-98.
**Yoshikawa, S., McKinnon, R. D., Kokel, M. and Thomas, J. B.** (2003). Wnt-mediated axon guidance via the Drosophila Derailed receptor. *Nature* **422**, 583-588.
**Yu, J., Chia, J., Canning, C. A., Jones, C. M., Bard, F. A. and Virshup, D. M.** (2014). WLS retrograde transport to the endoplasmic reticulum during Wnt secretion. *Dev. Cell* **29**, 277-291.

# A novel point-of-care system for high-speed real-time polymerase chain reaction testing for epidermal growth factor receptor mutations in bronchial lavage fluids after transbronchial biopsy in patients with non-small cell lung cancer

TOMOHIRO SAKAMOTO, MASAHIRO KODANI, MIYAKO TAKATA, HIROKI CHIKUMI, MASAKI NAKAMOTO, SHIZUKA NISHII-ITO, YASUTO UEDA, HIROKI IZUMI, HARUHIKO MAKINO, HIROKAZU TOUGE, KENICHI TAKEDA, AKIRA YAMASAKI, MASAAKI YANAI, NATSUMI TANAKA, TADASHI IGISHI and EIJI SHIMIZU

Division of Medical Oncology and Molecular Respirology, Faculty of Medicine, Tottori University, Yonago, Japan

Received October 23, 2014; Accepted December 10, 2014

DOI: 10.3892/ijo.2015.2875

**Abstract.** Epidermal growth factor receptor (*EGFR*) gene mutation testing is essential for choosing appropriate treatment options in patients with advanced non-small cell lung cancer (NSCLC). However, a time delay occurs between histological diagnosis and molecular diagnosis in clinical situations. To minimize this delay, we developed a novel point-of-care test for *EGFR* mutations, based on a high-speed real-time polymerase chain reaction (PCR) system designated here as ultrarapid PCR combined with highly accurate bronchoscopic sampling. We investigated whether our system for detecting *EGFR* mutations was valid by comparing test results with those obtained using a commercialized *EGFR* mutation test. We obtained small amounts of bronchial lavage fluids after transbronchial biopsies (TBBs) were performed on enrolled patients (n=168) who underwent endobronchial ultrasonography using a guide sheath (EBUS-GS). *EGFR* mutation analysis was performed by ultrarapid PCR immediately after EBUS-GS-TBBs were obtained (on the same day). After pathological diagnoses of NSCLC, *EGFR* mutation status in formalin-fixed, paraffin-embedded samples was confirmed by the PCR-invader method, and the concordance rates between the PCR methods were compared. The total diagnostic yield of EBUS-GS-TBB was 91.0%. The positive concordance rates for detecting 19del and L858R with the ultrarapid PCR and PCR-invader methods were both 100%. Negative concordance rates were 97.2 and 98.1%, respectively. We also demonstrated a dramatic effect of early erlotinib administration, based on ultrarapid PCR results, for a 52-year-old woman suffering from respiratory failure due to severe intrapulmonary metastases with poor performance status. In conclusion, ultrarapid PCR combined with EBUS-GS-TBB enabled rapid and reliable point-of-care testing for *EGFR* mutations.

*Correspondence to:* Dr Masahiro Kodani, Division of Medical Oncology and Molecular Respirology, Faculty of Medicine, Tottori University, 36-1 Nishi-machi, Yonago 683-8504, Japan
E-mail: kodani@med.tottori-u.ac.jp

*Key words:* ultrarapid PCR, *EGFR* mutation, point-of-care testing, virtual bronchoscopic navigation system, endobronchial ultrasonography using a guide sheath

## Introduction

Over the last decade, the discovery of epidermal growth factor receptor (*EGFR*) gene mutations and the development of tyrosine kinase inhibitors (TKIs) have dramatically changed the treatment strategies for patients with advanced non-small cell lung cancer (NSCLC) (1-5). Therefore, *EGFR* mutation testing is essential for optimal treatment selection for advanced NSCLC patients. Several methods for detecting *EGFR* mutations mainly in formalin-fixed, paraffin-embedded (FFPE) samples have already been validated and applied in practice (6-11). However, these methods adopt relatively complex polymerase chain reaction (PCR) technologies with predesigned fluorogenic probes, are packaged by manufacturers, and are often available through outside reference laboratories at relatively high rates. In Japan, the use of EGFR-TKIs for chemo-naïve patients has been limited to those with *EGFR* mutations since 2011. Despite this regulation, the majority of community and university hospitals still depend on outside laboratories for *EGFR* mutation testing. Accordingly, there is a time delay between histological diagnosis and molecular diagnosis in clinical situations. In general, obtaining PCR-based *EGFR* test results from outside laboratories requires 7-14 days after tumor sampling. In cases where immediate treatment is critical, failure to provide appropriate molecular targeted therapy due to delayed molecular diagnostic test results may cause fatal outcomes. Therefore, a quicker, simpler, and less expensive point-of-care *EGFR* mutation testing system is needed.

In the field of infectious diseases, a more rapid real-time PCR system for detecting pathogens has been developed (12). Similarly, we have developed a new, simple, high-speed

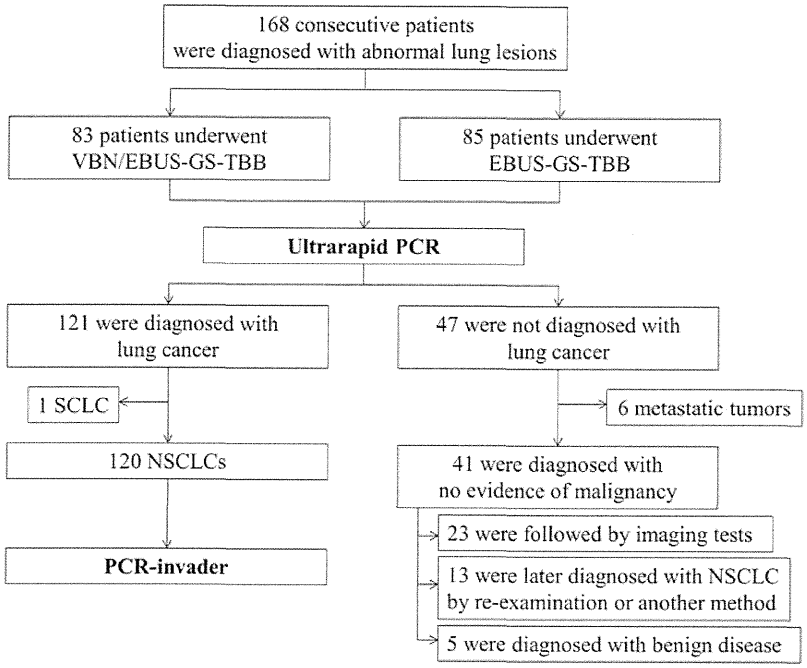


Figure 1. Flow diagram. One or more expert bronchoscopists determined whether to combine EBUS-GS with VBN, based on CT findings. For all 168 patients, analysis of *EGFR* mutations was performed by ultrarapid PCR immediately after the EBUS-GS-TBB procedure. A total of 121 patients (72%) were diagnosed with lung cancer by EBUS-GS-TBB. After a pathological diagnosis of NSCLC was made, *EGFR* mutation status was confirmed by the PCR-invader method. Thirteen patients (8%) who had not been diagnosed with NSCLC by EBUS-GS-TBB were later diagnosed with NSCLC by re-examination or by another sampling method.

real-time PCR system (referred to as ultrarapid PCR) for the detection of the 2 most common *EGFR* mutations. This assay involves a pair of mutation-specific primers used in combination with a newly developed PCR machine that is equipped with a novel thermo-control mechanism that makes ultrarapid PCR cycling possible.

In-frame deletion in exon 19 (E746-A750del) and the point mutation replacing leucine with arginine at codon 858 of exon 21 (L858R) represent >90% of oncogenic *EGFR* mutations. Large clinical trials have been conducted to establish the efficacy of EGFR-TKIs in targeting the resulting mutated EGFR proteins (1-5). Therefore, we designed a deletion-specific primer targeting the exon 19 E746-A750del mutation and a point mutation-specific primer for the exon 21 L858R mutation. PCR conditions were optimized for amplifying templates harboring each mutation.

Endobronchial ultrasonography using a guide sheath (EBUS-GS) combined with a virtual bronchoscopic navigation system (VBN) is very useful approach for collecting samples from peripheral pulmonary lesions (13-20). However, a major disadvantage of EBUS-GS is the low sample volume that can be obtained, leading to reduced sensitivity in molecular testing. Therefore, we performed this validation study to determine whether ultrarapid PCR can detect *EGFR* mutations with liquid bronchial lavage fluid (BLF) samples after EBUS-GS-transbronchial biopsies (EBUS-GS-TBBs) were taken.

## Materials and methods

*Patients and samples.* A total of consecutive 168 patients who underwent EBUS-GS-TBB at the Tottori University Hospital (Yonago, Japan) from November 2012 to December 2013 were enrolled prospectively (Fig. 1). Eligible patients had undiagnosed pulmonary lesions suspected to be lung cancer on chest computed tomography (CT) findings. Samples were prepared by mixing BLFs obtained during EBUS-GS-TBB procedures with saline solutions mixed with EBUS-GS-brush biopsy samples after they were stamped on glass slides. DNA was extracted from patient fluid samples using the QIAamp Blood Mini kit (Qiagen, Tokyo, Japan) (Fig. 2).

Ethical approval was obtained from the Tottori University Hospital and informed consent was obtained from all patients involved prior to performing bronchoscopies.

*VBN and EBUS-GS-TBB procedures.* VBNs were performed following approval from physicians and expert bronchoscopists, based on CT findings. CT scan data from multi-detector chest CTs (64- or 128-row; slice width, 0.5 mm) were acquired from all patients before EBUS-GS-TBB. Individual CT data sets from VBN/EBUS-GS group were transferred to a workstation on which VBN software (Bf-NAVI; Cybernet Systems, Co., Ltd., Tokyo, Japan) automatically created VBN images within 15 min. VBN images could be moved multi-directionally on a monitor beside the video-bronchoscopic monitor. All patients were anaesthetized with midazolam and examined using a P260F video bronchoscope (4.0 mm outer diameter; Olympus Corp., Tokyo, Japan). The bronchoscope was introduced into the targeted bronchus with VBN support or the guidance of 2 expert bronchoscopists based on CT axial images. Peripheral target lesions were visualized using a 20 MHz radial-type EBUS probe (external diameter, 1.4 mm; UM-S20-17S; Olympus) with a GS (K-201; Olympus) through

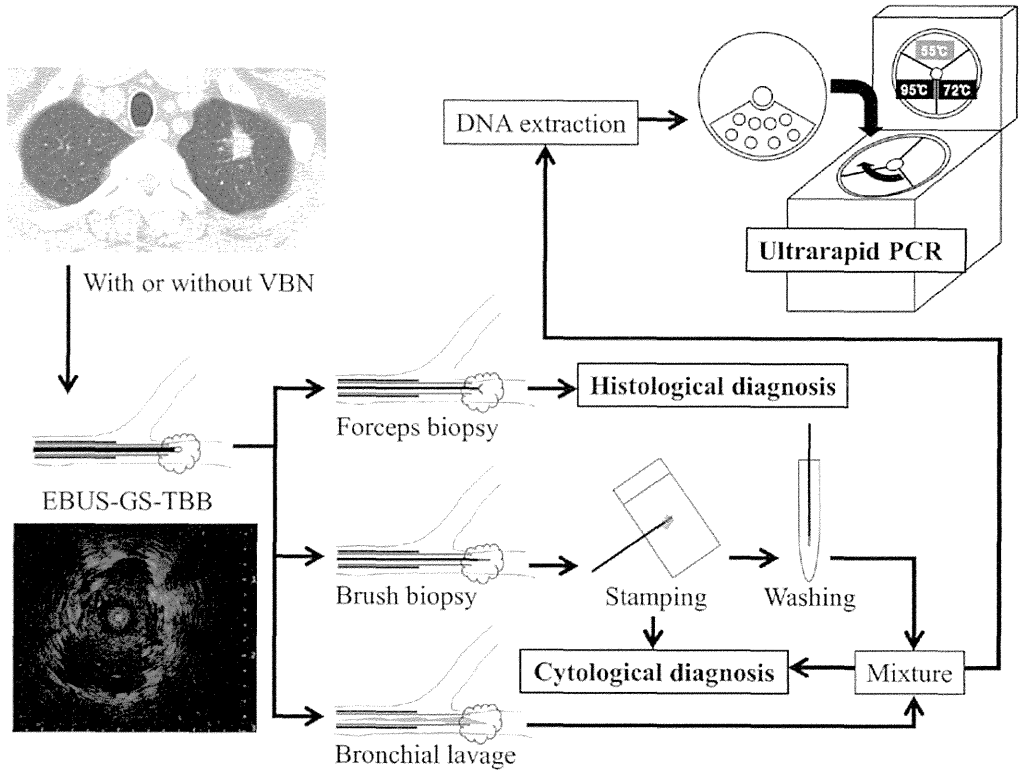


Figure 2. Examination flow chart. An EBUS probe with GS was led into the target lesion and adjusted with EBUS imaging. After removing the EBUS probe, forceps and brush biopsies were performed. At the end of the examinations, bronchial lavages were performed with 20 ml of saline. DNA was extracted from a mixture of bronchial lavage fluid and brush washings.

a working channel. Ultrasound images were processed in an ultrasound scanner (EU-ME-1 or EU-ME2; Olympus). Pathological samples were collected using forceps and brushes through the GS. Biopsy samples were immediately fixed in formalin. After biopsies were obtained, the target area was washed with 20 ml of saline.

*Mutation-specific PCR using an ultrarapid PCR machine.* *EGFR* exon 19 E746-A750 deletion type 1 (2235-2249del; 5'-GGAATTAAGAGAAGC-3') and exon 21 L858R (2573T>G) were detected using a novel high-speed real-time PCR machine, namely a Hyper-PCR UR104MK IV (Trust Medical Co., Ltd., Kasai, Japan), with allele-specific primers and SpeedSTAR HS DNA Polymerase (Takara Bio, Inc., Shiga, Japan). The UR104MK IV PCR machine utilized a novel temperature control technology. In this system, the PCR mixture is enclosed in a small vessel on a thin, flexible plastic disk and sealed with adhesive film, and the disk is rotated rapidly onto 3 separated heat elements. Rapid PCR can be accomplished by controlling the speed of rotation and the temperature of the 3 heat elements. The UR104MK also has the capacity for real-time monitoring of PCR reactions with a fluorescent probe and post-PCR melt curve analysis. The typical time for amplification and detection when using this machine was <10 min.

Optimized reaction mixtures contained 1.6 $\mu$l of 10X Fast buffer I (Takara), 1.3 $\mu$l of 2.5 mM dNTPs, 0.4 $\mu$l of each allele-specific primer (10 $\mu$M), 0.2 $\mu$l of SpeedSTAR HS DNA Polymerase (5 U/$\mu$l; Takara), 1 $\mu$l of template DNA, 1.6 $\mu$l of 1:2,000 SYBR-Green, and 9.5 $\mu$l of $ddH_2O$ in a volume of 16 $\mu$l. Furthermore, dimethylsulfoxide was added to obtain a final concentration of 5%. PCR thermal cycling conditions were as follows. To amplify E746-A750del type 1, we used 1 cycle of 94°C for 1 min, followed by 35 cycles of 98°C for 1.3 sec, 55°C for 5 sec, and 72°C for 3 sec. To amplify DNA sequences harboring the L858R point mutation, we used 1 cycle of 94°C for 1 min, followed by 30 cycles of 98°C for 1.3 sec, 68°C for 8 sec and 68°C for 8 sec.

*Sensitivity assay.* To validate the sensitivity of the PCR system, sensitivity assays were performed using DNA mixtures extracted from the following cell lines: PC9 (2235-2249del), H1975 (2573T>G) and N417 (wild-type). The PC9 cell line was obtained from the RIKEN Cell Bank (Tsukuba, Japan). The H1975 cell line was obtained from the American Type Culture Collection (Rockville, MD, USA). The N417 cell line was provided by Dr A.F. Gazdar and Dr H. Oie (National Cancer Institute-Navy Medical Oncology Branch, Bethesda, MD, USA). These cell lines were mixed in different ratios. Specifically, the PC9 and N417 cell lines were mixed in ratios of 1:0, 0.5:0.5, 0.1:0.9, 0.01:0.99 and 0:1, respectively, while the H1975 and N417 were mixed in ratios of 1:0, 0.5:0.5, 0.1:0.9, 0.01:0.99 and 0:1, respectively. Analysis of *EGFR* mutations was performed as described above.

*Comparison of ultrarapid PCR with the PCR-invader method.* *EGFR* mutation analysis was performed with BLF samples from all 168 patients, regardless of pathological diagnosis, by ultrarapid PCR immediately after EBUS-GS-TBB. After pathological diagnosis of NSCLC, the associated *EGFR*

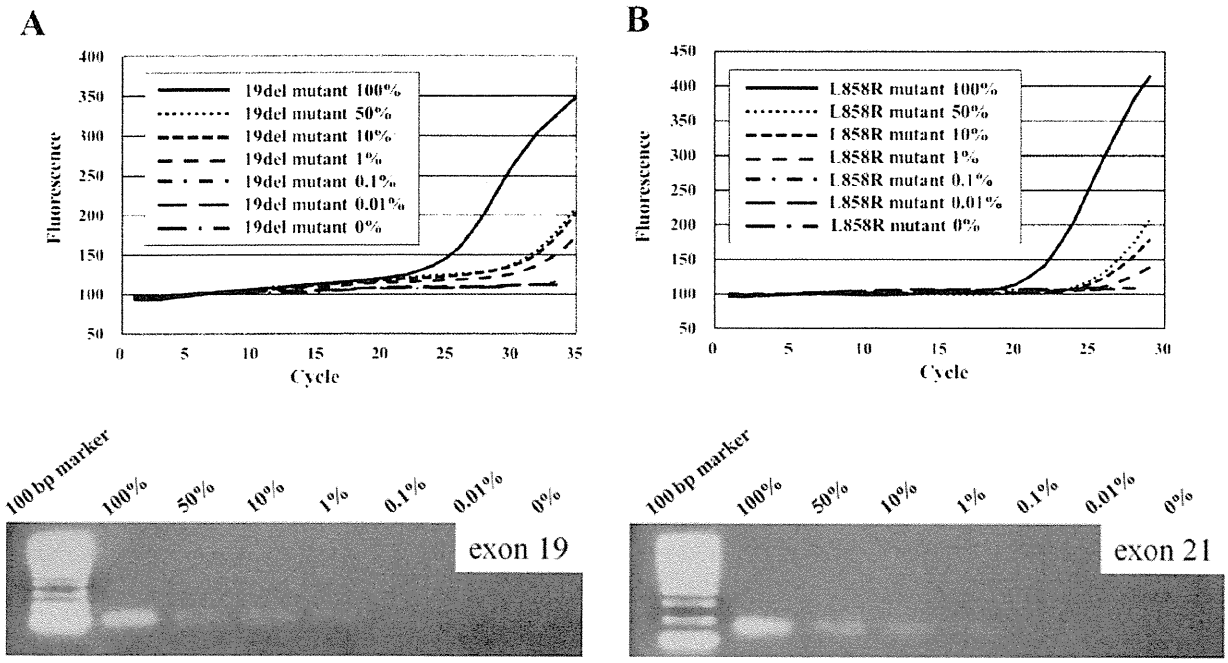


Figure 3. Sensitivity of ultrarapid PCR. (A) Amplification of the 19del allele by ultrarapid PCR was performed using cell samples containing 100, 50, 10, 1, 0.1, 0.01 and 0% PC14 cells, mixed with N417 cells containing 2 copies of the wild-type *EGFR* gene. As few as 1% of tumor cells with the 19del mutation could be detected. (B) Amplification of the L858R allele by ultrarapid PCR using cell samples containing 100, 50, 10, 1, 0.1, 0.01 and 0% H1975 cells, mixed with N417 cells. As few as 1% of tumor cells with L858R mutation could be detected.

mutation statuses in FFPE samples were evaluated by the PCR-invader method (BML, Inc., Tokyo, Japan), which is used in clinical practice at our hospital. To assess the performance of ultrarapid PCR, we evaluated the concordance rates and calculated kappa coefficients for both the ultrarapid PCR and PCR-invader methods.

*Statistical analysis.* Average target lesion diameters and diagnostic yields were calculated for the VBN/EBUS-GS and EBUS-GS groups, respectively, and analyzed using the Mann-Whitney U test and the Chi-squared test between these 2 groups. All P-values were 2-sided. A P-value of <0.05 indicated statistical significance. Concordance rates and Cohen's kappa coefficients were determined between the ultrarapid PCR and PCR-invader methods. Cohen's kappa coefficient was calculated as kappa = (Po-Pe)/(1-Pe), where Po is the observed concordance rate and Pe is the expected probability of chance agreement (21). A kappa of zero means that there is no agreement beyond chance, and a kappa of 1.00 means that there is perfect agreement. Values ranging from 0.81 to 1.00 indicate near perfect agreements (22). All data were statistically analyzed using IBM SPSS Statistics, ver. 22.

## Results

*Sensitivity.* The E746-A750del mutation was detected in mixed cell populations containing decreasing percentages (100-1%) of the E746-A750del-positive cell line (PC9) and increasing percentages of the N417 cell line containing 2 copies of the wild-type *EGFR* gene. Similarly, the L858R mutation was detected in cell line mixtures containing 100-1% of an L858R mutation-positive cell line (H1975) and N417 cells (Fig. 3).

*Characteristics of patients and patient samples.* VBN was combined with EBUS-GS for 83 out of the 168 patients enrolled in the present study. The median and average diameters of the target lesions were 25 and 30.6 mm, respectively (range, 8-150 mm). In the VBN/EBUS-GS group, the median and average diameters of target lesions were 19 and 20.5 mm, respectively (range, 8-54 mm). In the EBUS-GS group, the median and average diameters of target lesions were 34.5 and 38.6 mm, respectively (range, 8-150 mm; Table I). As shown in Fig. 1, lung cancer was diagnosed histologically in 121 patients, but not in 47 patients, including 5 patients with benign diseases and 6 patients with metastatic tumors. Thirteen out of the 41 patients who were not diagnosed with NSCLC using EBUS-GS-TBB specimens were later diagnosed with NSCLC by re-examination or using another sampling method. Twenty-three patients were provided follow-up with imaging examinations at fixed intervals, and did not show enlargement of peripheral small lesions after EBUS-GS-TBB. After these 23 patients were excluded from the analysis, the total diagnostic yield obtained with EBUS-GS-TBB samples was 91.0% (132/145 cases). In the EBUS-GS-TBB group, the diagnostic yield was 94.6% (70/74 cases), while the diagnostic yield of the VBN/EBUS-GS-TBB was 87.3% (62/71 cases; Table I). Although target lesion diameters were significantly different (P<0.001; Mann-Whitney U test), diagnostic yields were similar in the 2 groups (P=0.18; Chi-squared test).

The median age of the 121 lung cancer patients was 70 years (range, 37-97), and all of the patients were Japanese. NSCLC specimens were classified histologically as adenocarcinoma in 89 patients (73.6%), squamous cell carcinoma in 22 patients (18.2%), large-cell neuroendocrine carcinoma (LCNEC) in 4 patients (3.3%), adenosquamous carcinoma in 2

Table I. Comparison of target lesions diameters and diagnostic yields between VBN/EBUS-GS-TBB and EBUS-GS-TBB.

| | VBN/EBUS-GS-TBB (N=83) | EBUS-GS-TBB (N=85) | P-value |
|---|---|---|---|
| Diameter (mm) | | | |
| Median | 19.0 | 34.5 | |
| Average | 20.5 | 38.6 | <0.001[b] |
| Range | 8-54 | 8-150 | |
| Diagnostic yield[a] | 87.3% (62/71 cases) | 94.6% (70/74 cases) | 0.18[c] |

[a]The diagnostic yield of EBUS-GS-TBB was 91.0% (132/145). The diagnostic yield was calculated for all patients, except for 23 patients that were provided follow-up with imaging examinations at fixed intervals and for whom enlargement of peripheral small lesions after EBUS-GS-TBB was not observed. [b]Mann-Whitney U test; [c]Chi-squared test.

Table II. Patient characteristics.

| Characteristics | Diagnosed with lung cancer by EBUS-GS-TBB[a] (N=121) | Not diagnosed with lung cancer by EBUS-GS-TBB (N=47) |
|---|---|---|
| Age (years) | | |
| Median | 70 | 71 |
| Range | 37-97 | 65-87 |
| Male gender, n (%) | 75 (64.1) | 29 (56.9) |
| Smoking status, n (%) | | |
| Current smoker | 34 (28.1) | 7 (14.9) |
| Former smoker | 48 (39.7) | 22 (46.8) |
| Never smoker | 39 (32.2) | 18 (38.3) |
| Histologic type, n (%) | | |
| Adenocarcinoma | 89 (73.6) | |
| Squamous cell carcinoma | 22 (18.2) | |
| Large cell carcinoma | 2 (1.7) | |
| Small cell carcinoma | 1 (0.8) | |
| Adenosquamous carcinoma | 2 (1.7) | |
| LCNEC | 4 (3.3) | |
| Pleomorphic | 1 (0.8) | |
| Stage, n (%) | | |
| I | 60 (49.6) | |
| II | 13 (10.7) | |
| III | 15 (12.4) | |
| IV | 32 (26.4) | |
| Not evaluated | 1 (0.8) | |

[a]A total of 121 patients were diagnosed bronchoscopically with lung cancer. Out of 121 cancers, 89 (73.6%) were adenocarcinoma and 32 (26.4%) were stage IV.

patients (1.7%), large cell carcinoma in 2 patients (1.7%), small cell carcinoma in 1 patient (0.8%), and pleomorphic carcinoma in 1 patient (0.8%). The distribution of clinical stages at the time of diagnosis was as follows: 60 patients (49.6%) had stage I carcinoma, 13 patients (10.7%) had stage II, 15 patients (12.4%) had stage III, and 32 patients (26.4%) had stage IV. In 1 patient, the clinical stage was not classified (Table II).

Table III. Comparison of ultrarapid PCR and PCR-invader test results found when detecting the 2 most common *EGFR* mutations in samples from 120 NSCLC patients.

| | PCR-invader | | |
|---|---|---|---|
| Ultrarapid PCR | Mutation (+) | Mutation (-) | Total |
| 19del | | | |
| Mutation (+) | 11 | 0 | 11 |
| Mutation (-) | 3 | 106 | 109 |
| Total | 14 | 106 | 120 |
| L858R | | | |
| Mutation (+) | 15 | 0 | 15 |
| Mutation (-) | 2 | 103 | 105 |
| Total | 17 | 103 | 120 |

*EGFR mutation detection by ultrarapid PCR. EGFR* mutations in BLF samples were detected by ultrarapid PCR in 26 adenocarcinoma patients among the 120 NSCLC patients tested (21.7%), but were not detected in any of the 48 patients who were not diagnosed bronchoscopically with NSCLC. Eleven patients (42.3%) had an *EGFR* 19del mutation, and 15 patients (57.7%) had an L858R *EGFR* point mutation (Table III).

*Comparison of the ultrarapid PCR and PCR-invader detection methods. EGFR* mutations in FFPE tissues were detected in 36 adenocarcinoma patients among 120 NSCLC patients (30.0%) by the PCR-invader method (Table III). Two of these patients (5.6%) had an exon 18 G719A point mutation, 1 patient (2.8%) had a G719C point mutation and an exon 20 S768I point mutation, 1 patient (2.8%) had a G719S and a S768I mutation, 1 patient (2.8%) had a G719C mutation and an exon 21 L858R mutation, 8 patients (22.2%) had an E746-A750del type 1 mutation, 1 patient (2.8%) had an E746-A750del type 2

Table IV. Concordance rates and Cohen's kappa coefficients between the ultrarapid PCR and PCR-invader methods.

| Concordance rate | 19del (%) | L858 (%) |
|---|---|---|
| Positive | 100 | 100 |
| Negative | 97.2 | 98.1 |
| Kappa coefficient[a] | 0.87 | 0.93 |

[a]A range from 0.81 to 1.00 corresponds to near perfect agreement.

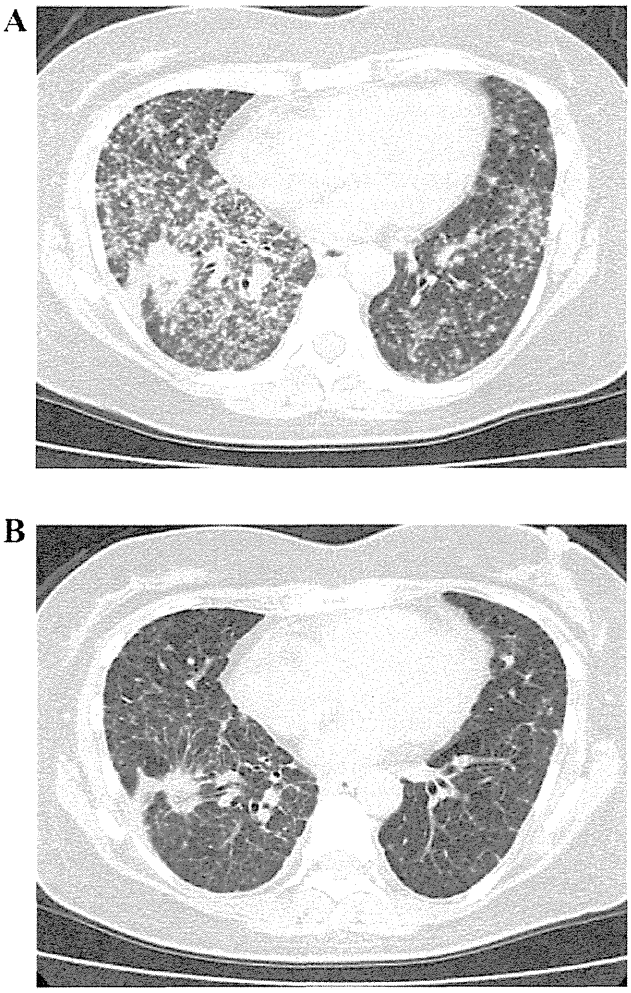


Figure 4. Dramatic effect of EGFR-TKI for a poor PS *EGFR* mutant. A chest CT scan obtained before treatment (A) and at 2 weeks after the administration of erlotinib (B) are shown. The diffuse granular shadow of the bilateral lung field had mostly disappeared after the initiation of therapy. Consequently, the patient's PS score improved from 3 to 1.

mutation, 6 patients (16.7%) had low-frequency mutations in exon 19, and 16 patients (44.4%) had an L858R mutation.

As shown in Table IV, positive concordance rates of 19del and L858R between ultrarapid PCR and PCR-invader were both 100%, while negative concordance rates were 97.2 and 98.1%, respectively. The kappa coefficients for detecting the 19del and L858R mutations between ultrarapid PCR and PCR-invader were 0.87 and 0.93, respectively. The average turnaround time for ultrarapid PCR was only 90 min, whereas that for the PCR-invader method by an outside laboratory was 9 days.

*Case report.* A 52-year-old non-smoking female, without previous illness, was admitted to our hospital because of a dry cough and dyspnea at rest. Her performance status (PS) was 3 on admission. Her chest CT scan showed numerous bilateral diffuse granular lung shadows and a 20 mm-diameter nodular shadow on the lower right lobe (Fig. 4A). Whole body bone scintigraphy was performed later, revealing an abnormal accumulation in the fifth lumbar vertebra. Suspecting that she had advanced lung cancer, we immediately performed an EBUS-GS-TBB against the primary lesion of the lower right lobe. By 60 min after performing the EBUS-GS-TBB procedure, we obtained a positive result for the E746-A750del mutation by ultrarapid PCR. Because she had respiratory failure and a poor PS on admission, she was not eligible for cytotoxic chemotherapy. Therefore, it was deemed appropriate to initiate EGFR-TKI therapy as soon as possible. The following day, we started EGFR-TKI therapy (erlotinib 150 mg orally every 24 h), after obtaining a definitive pathological diagnosis of adenocarcinoma by an immunohistochemical method. Two weeks later, the diffuse and numerous granular shadows of bilateral lung field had mostly disappeared (Fig. 4B). Moreover, her respiratory failure and poor PS score were dramatically improved before PCR-invader results were provided.

## Discussion

Bronchoscopy has been used to diagnose abnormal lung lesions for ~60 years. In recent years, the development of new diagnostic tools, such as EBUS, GS and VBN, has substantially improved diagnostic accuracy. Eberhardt *et al* (15) reported that the combination of EBUS and VBN improved the diagnostic yield in peripheral lung lesions, and VBN/EBUS is recommended for the diagnosis of lung peripheral lesions in guidelines of the European Society for Medical Oncology (23). Ishida *et al* (24) reported that the diagnostic yield of VBN combined EBUS-GS with small peripheral lesions (diameter <30 mm) was 80%. Similarly, we found high diagnostic yields in the present study despite the fact that most target lesions were small, especially in the VBN/EBUS-GS group. The appropriate decisions made regarding whether VBN should be used reinforced the diagnostic accuracy of EBUS-GS-TBBs for small peripheral lesions. Moreover, we usually collect at least 6 or more tissue samples. An advantage of EBUS-GS-TBB is that it is easy to obtain multiple biopsies through the fixed GS safely.

In this study, we validated ultrarapid PCR as a method for detecting the 2 most common *EGFR* mutations in liquid samples obtained by the EBUS-GS-TBB method. In many cases, even though these samples contain a very small amount of tumor cells, our method can detect the major *EGFR* mutations. Previous studies have shown similar results by molecular analysis of liquid samples collected by bronchoscopy. Yamaguchi *et al* (25) concluded that the analysis of *EGFR*, *KRAS* and *TP53* mutations using curette lavage fluids obtained by bronchoscopy was possible. Furthermore, some

reports have described the molecular analysis of lymph node samples obtained by EBUS guided trans-bronchial needle aspiration (26-28) or trans-esophageal ultrasound scanning with fine needle aspiration (29,30). Likewise, Buttitta *et al* (31) reported that *EGFR* mutation analysis of bronchoalveolar lavage by next-generation sequencing was possible even in cases where conventional methods failed. Importantly, the accuracy of our method was remarkably high, although the BLF samples contained a small amount of tumor cells.

The greatest advantage of the ultrarapid PCR method is its speed. To the best of our knowledge, ultrarapid PCR is the fastest PCR system for detecting *EGFR* mutations at present. Ultrarapid PCR is completed within 10 min, while other methods take a few hours to detect mutations. This advantage can potentially have positive effects on treatment outcomes in cases requiring urgent treatment by early EGFR-TKI administration. Generally, the administration of cytotoxic agents for patients with poor PS is not recommended (32). However, some reports indicate that the use of EGFR-TKIs in patients with poor PS is effective and feasible because of their relatively mild toxicities (33). It is necessary to be careful in selecting therapeutic measures because TKIs are associated with an increased risk for developing interstitial pneumonitis in patients with poor PS scores (34). In addition, it will also be important to explore therapeutic opportunities for improving prognoses.

Most *EGFR* mutations are located in exon 18, 19, 20 and 21, with ~90% of these mutations occurring in exons 19 and 21 (35). In previous phase III trials with EGFR-TKIs, patients with hotspot mutations (exon 19 deletions or exon 21 L858R) were mostly recruited. The response rate of patients with these hotspot mutations was ~80% (2,5). In contrast, the response rate of patients with minor mutations, such as exon 18 point mutation G719X and exon 21 point mutation L861Q, was only 20% (36). Moreover, EGFR-TKIs had no proven survival benefit in patients with minor mutations (36). Therefore, we limited our search to these hotspot mutations in this study.

As demonstrated in our case report, ultrarapid PCR can deliver quick results in practical clinical situations. Patients with hotspot mutations in need of immediate care should receive EGFR-TKI treatment as soon as possible. Failures in providing appropriate molecular therapy due to molecular diagnosis delays should be avoided.

Despite the promising results obtained using ultrarapid PCR for detecting major *EGFR* mutations, a limitation of this method is that it can only detect known mutations. Detecting minor *EGFR* mutations in exon 18 and the T790M point mutation associated with drug resistance (exon 20) will require the development of additional probes. This current limitation reduces patients' opportunities for rapid qualification for the third-generation EGFR-TKIs therapy, such as AZD9291 (37) by ultrarapid PCR alone. However, this problem may be solved by the development of additional primer sets for minor mutations in the near future.

In conclusion, it was demonstrated that ultrarapid PCR is an extremely quick and precise method for examining clinical liquid samples with a background of normal cells. The combination of ultrarapid PCR and EBUS-GS-TBB methods may enable point-of-care testing for NSCLC patient samples harboring *EGFR* mutations.

## References


1. Fukuoka M, Wu YL, Thongprasert S, *et al*: Biomarker analyses and final overall survival results from a phase III, randomized, open-label, first-line study of gefitinib versus carboplatin/paclitaxel in clinically selected patients with advanced non-small-cell lung cancer in Asia (IPASS). J Clin Oncol 29: 2866-2874, 2011.
2. Maemondo M, Inoue A, Kobayashi K, *et al*: Gefitinib or chemotherapy for non-small-cell lung cancer with mutated EGFR. N Engl J Med 362: 2380-2388, 2010.
3. Mitsudomi T, Morita S, Yatabe Y, *et al*: Gefitinib versus cisplatin plus docetaxel in patients with non-small-cell lung cancer harbouring mutations of the epidermal growth factor receptor (WJTOG3405): an open label, randomised phase 3 trial. Lancet Oncol 11: 121-128, 2010.
4. Paez JG, Janne PA, Lee JC, *et al*: *EGFR* mutations in lung cancer: correlation with clinical response to gefitinib therapy. Science 304: 1497-1500, 2004.
5. Zhou C, Wu YL, Chen G, *et al*: Erlotinib versus chemotherapy as first-line treatment for patients with advanced *EGFR* mutation-positive non-small-cell lung cancer (OPTIMAL, CTONG-0802): a multicentre, open-label, randomised, phase 3 study. Lancet Oncol 12: 735-742, 2011.
6. Asano H, Toyooka S, Tokumo M, *et al*: Detection of *EGFR* gene mutation in lung cancer by mutant-enriched polymerase chain reaction assay. Clin Cancer Res 12: 43-48, 2006.
7. Hoshi K, Takakura H, Mitani Y, *et al*: Rapid detection of epidermal growth factor receptor mutations in lung cancer by the SMart-Amplification Process. Clin Cancer Res 13: 4974-4983, 2007.
8. Hall JG, Eis PS, Law SM, *et al*: Sensitive detection of DNA polymorphisms by the serial invasive signal amplification reaction. Proc Natl Acad Sci USA 97: 8272-8277, 2000.
9. Nagai Y, Miyazawa H, Huqun, *et al*: Genetic heterogeneity of the epidermal growth factor receptor in non-small cell lung cancer cell lines revealed by a rapid and sensitive detection system, the peptide nucleic acid-locked nucleic acid PCR clamp. Cancer Res 65: 7276-7282, 2005.
10. Naoki K, Soejima K, Okamoto H, *et al*: The PCR-invader method (structure-specific 5' nuclease-based method), a sensitive method for detecting EGFR gene mutations in lung cancer specimens; comparison with direct sequencing. Int J Clin Oncol 16: 335-344, 2011.
11. Sasaki H, Endo K, Konishi A, *et al*: *EGFR* mutation status in Japanese lung cancer patients: genotyping analysis using LightCycler. Clin Cancer Res 11: 2924-2929, 2005.
12. Fujimoto T, Konagaya M, Enomoto M, *et al*: Novel high-speed real-time PCR method (Hyper-PCR): results from its application to adenovirus diagnosis. Jpn J infect Dis 63: 31-35, 2010.
13. Asahina H, Yamazaki K, Onodera Y, Kikuchi E, Shinagawa N, Asano F and Nishimura M: Transbronchial biopsy using endobronchial ultrasonography with a guide sheath and virtual bronchoscopic navigation. Chest 128: 1761-1765, 2005.
14. Asano F, Matsuno Y, Shinagawa N, Yamazaki K, Suzuki T, Ishida T and Moriya H: A virtual bronchoscopic navigation system for pulmonary peripheral lesions. Chest 130: 559-566, 2006.
15. Eberhardt R, Anantham D, Ernst A, Feller-Kopman D and Herth F: Multimodality bronchoscopic diagnosis of peripheral lung lesions: a randomized controlled trial. Am J Respir Crit Care Med 176: 36-41, 2007.
16. Eberhardt R, Kahn N, Gompelmann D, Schumann M, Heussel CP and Herth FJ: LungPoint - a new approach to peripheral lesions. J Thorac Oncol 5: 1559-1563, 2010.
17. Fielding DI, Chia C, Nguyen P, Bashirzadeh F, Hundloe J, Brown IG and Steinke K: Prospective randomised trial of endobronchial ultrasound-guide sheath versus computed tomography-guided percutaneous core biopsies for peripheral lung lesions. Intern Med J 42: 894-900, 2012.
18. Gildea TR, Mazzone PJ, Karnak D, Meziane M and Mehta AC: Electromagnetic navigation diagnostic bronchoscopy: a prospective study. Am J Respir Crit Care Med 174: 982-989, 2006.
19. Seijo LM, de Torres JP, Lozano MD, Bastarrika G, Alcaide AB, Lacunza MM and Zulueta JJ: Diagnostic yield of electromagnetic navigation bronchoscopy is highly dependent on the presence of a Bronchus sign on CT imaging: results from a prospective study. Chest 138: 1316-1321, 2010.

20. Kurimoto N, Miyazawa T, Okimasa S, Maeda A, Oiwa H, Miyazu Y and Murayama M: Endobronchial ultrasonography using a guide sheath increases the ability to diagnose peripheral pulmonary lesions endoscopically. Chest 126: 959-965, 2004.
21. Kundel HL and Polansky M: Measurement of observer agreement. Radiology 228: 303-308, 2003.
22. Landis JR and Koch GG: The measurement of observer agreement for categorical data. Biometrics 33: 159-174, 1977.
23. Vansteenkiste J, De Ruysscher D, Eberhardt WE, Lim E, Senan S, Felip E, Peters S; ESMO Guidelines Working Group: Early and locally advanced non-small-cell lung cancer (NSCLC): ESMO Clinical Practice Guidelines for diagnosis, treatment and follow-up. Ann Oncol 24 (Suppl 6): vi89-vi98, 2013.
24. Ishida T, Asano F, Yamazaki K, *et al*: Virtual bronchoscopic navigation combined with endobronchial ultrasound to diagnose small peripheral pulmonary lesions: a randamized trial. Thorax 66: 1072-1077, 2011.
25. Yamaguchi F, Kugawa S, Tateno H, Kokubu F and Fukuchi K: Analysis of *EGFR*, *KRAS* and *P53* mutations in lung cancer using cells in the curette lavage fluid obtained by bronchoscopy. Lung Cancer 78: 201-206, 2012.
26. Jurado J, Saqi A, Maxfield R, *et al*: The efficacy of EBUS-guided transbronchial needle aspiration for molecular testing in lung adenocarcinoma. Ann Thorac Surg 96: 1196-1202, 2013.
27. Santis G, Angell R, Nickless G, Quinn A, Herbert A, Cane P, Spicer J, Breen R, McLean E and Tobal K: Screening for *EGFR* and *KRAS* mutations in endobronchial ultrasound derived transbronchial needle aspirates in non-small cell lung cancer using COLD-PCR. PLoS One 6: e25191, 2011.
28. Tsai TH, Yang CY, Ho CC, *et al*: Multi-gene analyses from waste brushing specimens for patients with peripheral lung cancer receiving EBUS-assisted bronchoscopy. Lung Cancer 82: 420-425, 2013.
29. Lewandowska MA, Jozwicki W, Jochymski C and Kowalewski J: Application of PCR methods to evaluate *EGFR*, *KRAS* and *BRAF* mutations in a small number of tumor cells in cytological material from lung cancer patients. Oncol Rep 30: 1045-1052, 2013.
30. van Eijk R, Licht J, Schrumpf M, *et al*: Rapid *KRAS*, *EGFR*, *BRAF* and *PIK3CA* mutation analysis of fine needle aspirates from non-small-cell lung cancer using allele-specific qPCR. PLoS One 6: e17791, 2011.
31. Buttitta F, Felicioni L, Del Grammastro M, *et al*: Effective assessment of *egfr* mutation status in bronchoalveolar lavage and pleural fluids by next-generation sequencing. Clin Cancer Res 19: 691-698, 2013.
32. Pfister DG, Johnson DH, Azzoli CG, *et al*: American Society of Clinical Oncology treatment of unresectable non-small-cell lung cancer guideline: update 2003. J Clin Oncol 22: 330-353, 2004.
33. Inoue A, Kobayashi K, Usui K, *et al*: First-line gefitinib for patients with advanced non-small-cell lung cancer harboring epidermal growth factor receptor mutations without indication for chemotherapy. J Clin Oncol 27: 1394-1400, 2009.
34. Kudoh S, Kato H, Nishiwaki Y, *et al*: Interstitial lung disease in Japanese patients with lung cancer: a cohort and nested case-control study. Am J Respir Crit Care Med 177: 1348-1357, 2008.
35. Mitsudomi T and Yatabe Y: Mutations of the epidermal growth factor receptor gene and related genes as determinants of epidermal growth factor receptor tyrosine kinase inhibitors sensitivity in lung cancer. Cancer Sci 98: 1817-1824, 2007.
36. Watanabe S, Minegishi Y, Yoshizawa H, *et al*: Effectiveness of gefitinib against non-small-cell lung cancer with uncommon EGFR mutations G719X and L861Q. J Thorac Oncol 9: 189-194, 2014.
37. Cross DA, Ashton SE, Ghiorghiu S, *et al*: AZD9291, an irreversible EGFR TKI, overcomes T790M-mediated resistance to EGFR inhibitors in lung cancer. Cancer Dicov 4: 1046-1061, 2014.

# A new rapid method for detecting epidermal growth factor receptor mutations in non-small cell lung cancer

MIYAKO TAKATA[1], HIROKI CHIKUMI[1,2], KEIJI MATSUNAMI[1], MASAHIRO KODANI[1], TOMOHIRO SAKAMOTO[1], KAZUHIRO HASHIMOTO[3], MASAKI NAKAMOTO[1,2], KENSAKU OKADA[1], TSUYOSHI KITAURA[1], SHINGO MATSUMOTO[4], JUN KURAI[1], AKIRA YAMASAKI[1], TADASHI IGISHI[1], NAOTO BURIOKA[1,5] and EIJI SHIMIZU[1]

[1]Division of Medical Oncology and Molecular Respirology, Department of Multidisciplinary Internal Medicine, Tottori University, Yonago-shi, Tottori-ken; [2]Center for Infectious Diseases, Tottori University Hospital, Yonago-shi, Tottori-ken; [3]Trust Medical Co., Ltd., Hyogo; [4]Exploratory Oncology Research and Clinical Trial Center, National Cancer Center, Kashiwa, Chiba; [5]Department of Pathobiological Science and Technology, School of Health Science, Tottori University, Yonago-shi, Tottori-ken, Japan

Received October 20, 2014; Accepted December 5, 2014

DOI: 10.3892/or.2015.3716

**Abstract.** Mutations in the epidermal growth factor receptor (*EGFR*) gene are associated with a favorable clinical response to the EGFR tyrosine kinase inhibitors gefitinib and erlotinib in non-small cell lung cancer (NSCLC). We present here, a new method for the rapid detection of the two most common *EGFR* mutations (delE746-A750 and L858R) from clinical samples. The methodology involves the combination of newly designed mutation-specific primers and a novel real-time PCR machine with an innovative thermo-control mechanism that enables ultrarapid PCR. We evaluated this method using a cell mixture composed of various ratios of lung cancer cells harboring mutated or wild-type *EGFR*, lung cancer tissues obtained by surgery, and a cytology sample obtained by bronchoscopy from a lung cancer patient. In the cell mixture analysis, our method detected 0.1% of cells with delE746-A750 and 1% of cells with L858R among cells with wild-type *EGFR*. In 143 lung cancer tissues, the result of this assay was concordant with those of direct sequencing in 138 samples. The five samples with discordant results were tested using a PCR-Invader assay and the result matched those of our method at 100%. We also successfully detected *EGFR* mutations in the lavage obtained from a lung cancer patient. The turnaround time for this method was <10 min, and all steps could be accomplished in <50 min after sample collection. Thus, our novel PCR method offers a rapid, simple, and less expensive test for *EGFR* mutations and can be applied as a point-of-care diagnostic test.

*Correspondence to:* Professor Hiroki Chikumi, Division of Medical Oncology and Molecular Respirology, Department of Multidisciplinary Internal Medicine, Faculty of Medicine, Tottori University, 36-1 Nishi-machi, Yonago-shi, Tottori-ken 683-8504, Japan
E-mail: chikumi@grape.med.tottori-u.ac.jp

*Key words:* ultrarapid PCR, EGFR mutations, non-small cell lung cancer, epidermal growth factor receptor

## Introduction

Lung cancer is the leading cause of death from cancer globally (1). Non-small cell lung cancer (NSCLC) accounts for more than 80% of all lung cancer cases. Few NSCLC patients are diagnosed at an early stage and patients with advanced disease are treated with platinum-based combination chemotherapy; however, the objective response rate is very low (2). Resent advances in understanding the molecular basis of lung cancer has led to practical implementation of epidermal growth factor receptor (EGFR)-targeted treatment. The EGFR tyrosine kinase inhibitor (TKI) gefitinib was approved for the treatment of NSCLC in Japan in January 2002, and activating somatic mutations in *EGFR*, conferring sensitivity to EGFR TKIs were discovered in 2004 (3). Since then, EGFR TKIs, such as gefitinib and the equally effective erlotinib, have become the first-line treatment option for NSCLC patients in which the tumor harbors activating *EGFR* mutations, based on the results of a number of phase III trials (4-9). Therefore, in modern clinical settings, *EGFR* mutation testing has become essential for offering the most suitable therapy for a patient with advanced NSCLC.

The historical standard for *EGFR* mutation testing has been direct sequencing of DNA extracted from samples of resected tumor or from biopsies. This method is advantageous as it can be applied to discover 'new' mutations; to date, nearly 30 mutations in exons 18-21 have been detected in lung cancer specimens (3,10-14). However, direct sequencing has several limitations. The method requires complex steps and a few days to obtain a result. More importantly, the sensitivity of this method is low; mutant DNA must comprise ~20% of all the DNA in a sample in order to be reliably detected (15). Therefore, when the diagnosis is based on cytology samples

that contain a very low percentage of tumor cells, direct sequencing is not applicable.

More recently, based on findings that the most common *EGFR* mutations are a 15-bp in-frame deletion in exon 19 (delE746-A750) and a point mutation in exon 21 (L858R), which together account for ~90% of cases with *EGFR* mutations (16), more focused and mutation-specific approaches have been developed. These methods, PCR-Invader (17,18), peptide nucleic acid-locked nucleic acid (PNA-LNA) PCR clamp (19), cycleave PCR (20), and Scorpion Amplification Refractory Mutation System (ARMS) (21) are PCR-based methods that can detect known *EGFR* mutations with higher sensitivity and a shorter turnaround time than direct sequencing. Therefore, these methods are now frequently used in modern clinical laboratory practice.

However, these methods still have several limitations. These methods adopt relatively complex PCR technologies with pre-designed fluorogenic probes, are packaged by manufacturers, and are often available through outside reference laboratories at relatively expensive rates. The turnaround time for receiving results is 3-5 days, which can sometimes create a bottleneck for immediately starting TKI therapy in patients. Moreover, the cost of the testing renders repeated examination impossible; yet, this may sometimes be required for patients in whom the disease recurs after prior TKI therapy. Therefore, more rapid and less expensive *EGFR* mutation testing is required.

Here, we developed a new, simple, PCR-based method for the detection of the two most common *EGFR* mutations. This assay involves a pair of mutation-specific primers used in combination with a newly developed PCR machine that is equipped with a novel thermo-control mechanism that makes ultrarapid PCR cycling possible. In the present study, we evaluated this approach for *EGFR* mutation detection in tumor tissue gathered during resection and showed the feasibility of using this approach in a cytology sample collected by bronchoscopic examination.

## Materials and methods

*Cell lines and DNA samples.* All lung cancer cell lines used in the present study originated from adenocarcinoma. The 11-18 cell line was obtained from the Cell Resource Center for Biomedical Research (Tohoku University, Sendai, Japan). The Ma1 cell line was provided by Dr Hirashima (Osaka Prefectural Habikino Hospital, Osaka, Japan). The A549 cell line was purchased from the American Type Culture Collection (Rockville, MD, USA). The *EGFR* mutation status of these cell lines was examined in our previous study (22). Cells were maintained in DMEM (Wako, Osaka, Japan) supplemented with 10% fetal bovine serum (Life Technologies, Carlsbad, CA, USA), 50 U/ml penicillin, and 50 U/ml streptomycin (both from Wako). Genomic DNA was prepared using a Wizard® Genomic DNA Purification kit (A1120; Promega, Madison, WI, USA) according to the manufacturer's instructions.

*Clinical samples.* Ethical approval was obtained from the Tottori University Hospital and fully informed written consent was obtained from all patients involved prior to the surgery or tissue collection.

Tumor tissues were obtained from surgical specimens of resected tumors, from 143 lung cancer patients treated at Tottori University Hospital; these samples were embedded in Tissue-Tek OCT Compound (Sakura Finetechnical, Tokyo, Japan), and were immediately frozen at -80°C. Macrodissection of the OCT-embedded tissue samples was performed to enrich the final proportion of the tumor DNA, and DNA was extracted using the Wizard® Genomic DNA Purification kit. For samples with discordant results between direct sequencing and mutation-specific PCR, a PCR-Invader method was performed by BML, Inc. (Tokyo, Japan) as a reference test.

*Direct sequence analysis.* For direct sequence analysis exon 19 and 21 of *EGFR*, the following PCR primers were used: *EGFR* exon 19F, 5'-GCAATATCAGCCTTAGGTGCGGCTC-3' and *EGFR* exon 19R, 5'-CATAGAAAGTGAACATTTAGGATGTG-3'; and *EGFR* exon 21F, 5'-CTAACGTTCGCCAGCCATAAGTCC-3' and *EGFR* exon 21R, 5'-GCTGCGAGCTCACCCAGAATGTCTGG-3'. The PCR conditions were as follows: 1 cycle at 94°C for 9 min, followed by 40 cycles each consisting of 94°C for 1 min, 57°C for 1 min, and 72°C for 2 min, and a final cycle at 72°C for 5 min. The PCR products were purified with a MultiScreen-PCR filter plate (Millipore, Tokyo, Japan) and then sequenced using a BigDye Terminator v3.1 cycle sequencing kit and an ABI PRISM 3130xl genetic analyzer (Applied Biosystems, Foster City, CA, USA).

*Design of mutation-specific PCR primer sets.* We designed a deletion-specific primer for the delE746-A750 mutation within exon 19 and a point mutation-specific primer for the L858R mutation within exon 21 of *EGFR*. Sequences of the primer sets were as follows: PCR forward primer for delE746-A750, 5'-CACAATTGCCAGTTAACGTCTTC-3' (19DF) and PCR reverse primer for delE746-A750, 5'-TGTTGGCTTTCGGAGATGTTTTG-3' (19DR3); PCR forward primer for L858R, 5'-TCCCATGATGATCTGTCCCT-3' (21F2f) and PCR reverse primer for L858R, 5'-CACCCAGCAGTTTGGTCC-3' (21ARMS3).

*Mutation-specific PCR using a conventional thermal cycler.* For conventional PCR amplification using the mutation-specific primer sets, PCR conditions were as follows: the reaction mixtures contained 2 $\mu$l of 10X PCR buffer, 0.5 $\mu$l of dNTPs, 1 $\mu$l of each allelic-specific primer (10 $\mu$M), 0.2 $\mu$l of AmpliTaq® Gold DNA polymerase (Applied Biosystems), 1 $\mu$l of template DNA, and 14.3 $\mu$l of $ddH_2O$ in a total volume of 20 $\mu$l. Thermal cycling conditions on a PCR Thermal Cycler Dice (Takara, Shiga, Japan) were as follows for the delE746-A750 mutation: 1 cycle at 94°C for 9 min, followed by 35 cycles each consisting of 94°C for 1 min, 59°C for 1 min, and 72°C for 2 min, and a final cycle at 72°C for 5 min. Similarly, for the L858R mutation, conditions involved 1 cycle at 94°C for 9 min, followed by 35 cycles at 94°C for 1 min, 64°C for 1 min, and 72°C for 2 min, and a final cycle at 72°C for 5 min. The PCR products were then electrophoresed on agarose gels and stained with ethidium bromide.

*Mutation-specific PCR using an ultrarapid PCR machine.* For ultrarapid PCR-based *EGFR* mutation detection, we utilized a newly developed high-speed real-time PCR machine, termed

the 'Hyper-PCR' UR104MK III (Trust Medical, Hyogo, Japan), which was jointly developed by ourselves and Trust Medical (23). The UR104MK III employs a novel temperature control technology. In this system, the PCR mixture is enclosed in a small vessel on a thin, flexible plastic disk and sealed with adhesive film, and the disk is rotated rapidly onto three separated heat elements. By controlling the speed of rotation and the temperature of the three heat elements, rapid PCR can be accomplished. Real-time monitoring of the fluorescent dsDNA dye produced during PCR progression, and the ability to perform melting curve analysis of the PCR product are also incorporated into this machine (Fig. 1). The typical time for amplification and detection when using this apparatus is <10 min.

The optimized reaction mixtures for use with this machine contained 1.6 $\mu$l of 10X Fast Buffer I, 1.3 $\mu$l of a 2.5 mM dNTP mixture, 0.4 $\mu$l of each allele-specific primer (10 $\mu$M), 0.2 $\mu$l of SpeedSTAR HS DNA Polymerase (5 U/$\mu$l) (Takara), 1 $\mu$l of template DNA, 1.6 $\mu$l of 1:2,000 SYBR®-Green I nucleic acid gel stain (Cambrex Biosciences, Rockland, ME, USA), and 9.5 $\mu$l of $ddH_2O$ in a total volume of 16 $\mu$l. Furthermore, dimethyl sulfoxide (DMSO) Hybri-Max® (Sigma, St. Louis, MO, USA) was added to a final concentration of 5%. Thermal cycling conditions for ultrarapid PCR were as follows for the delE746-A750 mutation: 1 cycle at 94°C for 1 min, followed by 35 cycles each including 98°C for 1.30 sec, 55°C for 5.00 sec, and 72°C for 3.00 sec. Similarly, for the L858R mutation, conditions entailed 1 cycle at 94°C for 1 min, followed by 30 cycles each consisting of 98°C for 1.30 sec, 68°C for 8.00 sec, and a further 68°C for 8.00 sec. Total PCR cycling time for the delE746-A750 and the L858R mutation detection was within 6 and 9 min, respectively. Following PCR cycling, melting curve analysis was performed within 4 min.

For interpretation of the ultrarapid PCR results, criteria used in other studies of qualitative real-time PCR analysis were applied (24). In brief, to be considered as a positive result, a fluorescence signal generated during ultrarapid PCR should display an exponential amplification above the threshold level and the obvious crossing point (Cp) (25), with a single peak upon melting curve analysis, giving a unique melting temperature (Tm) value. A signal was considered as negative when no Cp value was obtained within the amplification cycles.

## Results

*Establishment of EGFR mutation-specific ultrarapid PCR.* We first established a specific PCR to detect mutations within exons 19 and 21 of *EGFR*, which are representative mutations underlying the responsiveness of NSCLC to EGFR inhibitors (3). The genomic sequence of *EGFR* was retrieved from the NCBI database (NM_005228). For the in-frame deletion within exon 19, which removes nucleotides 2235-2249, causing a deletion of amino acids 746 through 750 (delE746-A750), we designed a deletion-specific primer, 19DR3 (Fig. 2A). This primer was designed to anneal only to the genomic sequence harboring the nucleotide 2235-2249 deletion, by connecting the flanking sequences on either side of the deletion. By shortening the 3'-end of the primer that corresponded to the upstream genomic sequence, we could improve the specificity of the primer.

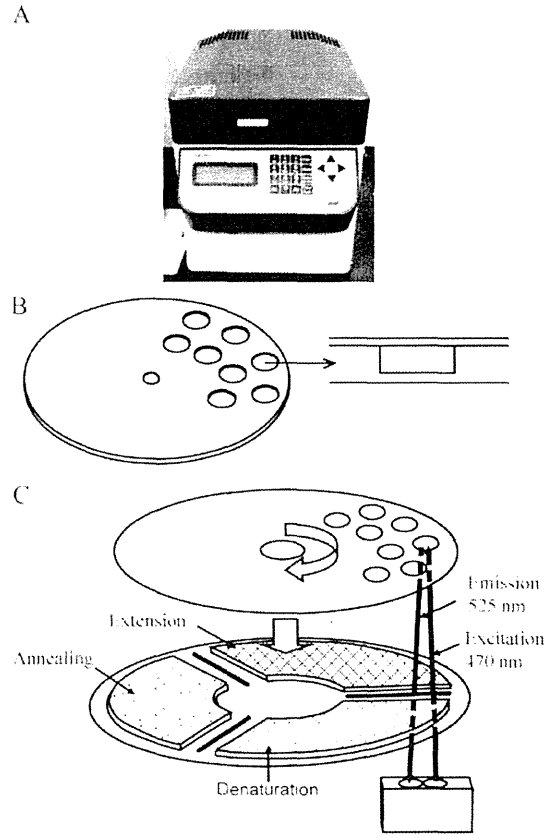


Figure 1. Architecture of the ultrarapid real-time PCR, UR104MK III. (A) External appearance of the machine. (B) A PCR reaction mixture is pipetted onto a flat well in a plastic disk, and sealed with thin film. (C) By high-speed rotation of the disk onto 3 independently controlled thermo-elements, ultrarapid PCR can be accomplished in <10 min. Fluorescence occurring with the production of PCR products is automatically monitored during each cycle, and immediately after ultrarapid PCR, melting curve analysis can be performed to verify product purity.

For the exon 21 amino acid substitution, in which G is substituted for T at nucleotide 2573, causing an amino acid substitution of L to R (L858R), a point mutation-specific primer, 21ARMS3, was designed (Fig. 2B). Here, we employed the ARMS technique, and designed the primers to be refractory to PCR amplification of non-matching target sequences (26,27), by also including an additional mismatch in the candidate point mutation-specific primers (ARMS1-10) at positions -2 or -3 from the 3'-end of the primers (data not shown). Among these candidate primers, we chose the primer (ARMS3) that allowed discrimination without decreasing the sensitivity and specificity of amplification in a series of experiments in which these candidate primers were tested under the same temperature and time conditions in ultrarapid PCR.

The forward primers for each mutation-specific primer were designed to match the stable area of each *EGFR* (19F and 21F). The concentration of the PCR primers and magnesium, the annealing temperature and other cycling parameters, and the type of DNA polymerase used were determined by exploration, and the conditions described here are the final optimized conditions.

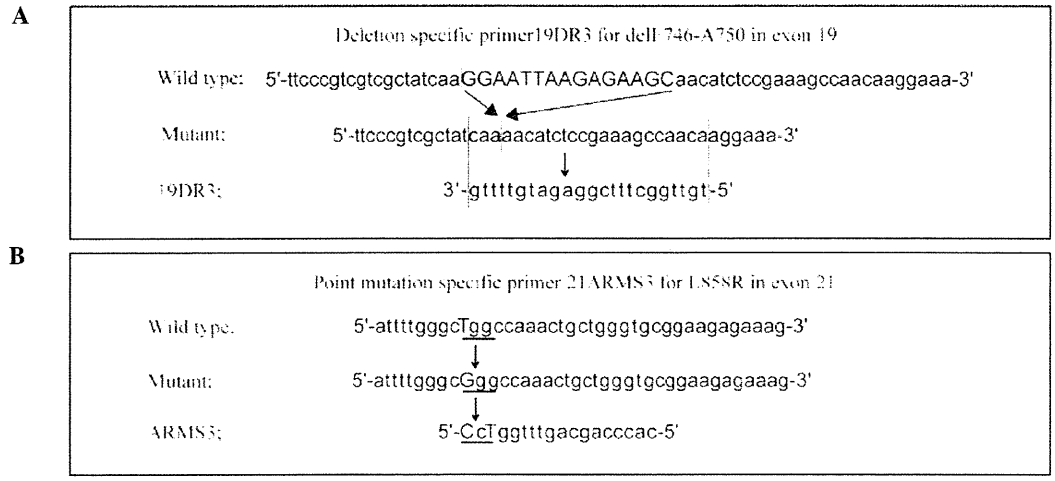


Figure 2. Mutation-specific primers. (A) The reverse primer specific for delE746-A750 in exon 19 (19DR3) was designed to anneal only to the genome containing a deletion of nucleotides 2235-2249, by connecting the regions flanking the deleted sequence. (B) The reverse primer specific for L858R in exon 21 (ARMS3) was designed to be homologous to nucleotides 2573-2590 of the mutant allele. An additional mismatch (C to T substitution) at the -2 position from the 3'-end of the primer was introduced to improve discriminatory ability. The forward primer for each mutation was designed to be homologous to the stable area of each exon.

*Specificity of the mutation-specific primers.* To evaluate the specificity of the mutation-specific primers, ultrarapid PCR using the mutation-specific primers was performed on lung cancer cell lines, and the concordance of these results with those of conventional PCR was evaluated. *EGFR* genotyping of the lung cancer cell lines Mal, 11-18 and A549 had been performed by sequence analysis in our previous study, and were revealed as delE746-A750, L858R and wild-type, respectively (22). As shown in Fig. 3A, using primer sets, 19DF and 19DR3, a significant increase in fluorescence intensity was observed upon ultrarapid PCR only in Mal cells that harbor delE746-A750, and melting curve analysis revealed a clear peak at the expected Tm (81.3°C). The PCR product was visualized by agarose gel electrophoresis and the expected product of 113 bp was detected. To validate the data, conventional PCR was performed using the same primer sets, and a product of the same size was detected only in Mal cells (Fig. 3B).

A similar experiment was performed using the L858R point mutation-specific primers (21F2f and 21ARMS3) in ultrarapid PCR. As shown in Fig. 3C, a significant increase in fluorescence intensity and a clear melting curve peak at the expected Tm (87.1°C) was observed only in 11-18 cells that harbor the exon 21 L858R point mutation, and the size of the amplicon was confirmed as 166 bp by agarose gel electrophoresis. The same result was obtained by conventional PCR using this primer set (Fig. 3D). These data revealed that the combination of mutation-specific primers and ultrarapid PCR yielded satisfactory discrimination of the mutant alleles.

*Sensitivity of mutation-specific PCR.* To evaluate the sensitivity of the assay, a serial dilution of lung cancer cell lines carrying *EGFR* mutations (Mal or 11-18) into wild-type cell lines (A549) was analyzed by ultrarapid PCR using the mutation-specific primers. Using the delE746-A750 primers in ultrarapid PCR, a mixture containing 0.1% Mal cells could be detected as positive from the amplification curve and melting curve analysis, and this result was confirmed by gel electrophoresis (Fig. 4A). The same result was also obtained by conventional PCR (Fig. 4B). Using the L858R primer sets, a cell mixture containing 1% 11-18 cells was detected as positive by ultrarapid PCR, and the result was confirmed by gel electrophoresis of the PCR product (Fig. 4C). The same detection limit was also observed with this primer set with conventional PCR (Fig. 4D). These data revealed that ultrarapid PCR combined with delE746-A750 and L858R mutation-specific primers allowed detection of 0.1 or 1% mutation-carrying lung cancer cells among wild-type cells, respectively.

*Clinical sample testing.* We evaluated the concordance of the results obtained by direct sequencing and using mutation-specific primers in ultrarapid PCR or conventional PCR in 143 lung cancer tumors. Overall, the results of 138 of 143 samples were concordant among direct sequencing, ultrarapid and conventional PCR (Fig. 5). The remaining five samples that demonstrated inconsistent results are shown in Table I. In these samples, direct sequencing could not detect any mutations, whereas the results with ultrarapid PCR and conventional PCR were concordant: two delE746-A750 and three L858R mutations were identified. To evaluate these discrepant samples, we used PCR-Invader analysis, which confirmed the PCR-based results. Therefore, we concluded that the indicated mutations were indeed present in these samples, yet could not be detected by direct sequencing, possibly due to the lower sensitivity of detection of direct sequencing methodology.

When compared with the concluded *EGFR* mutation status, the sensitivity and specificity of direct sequencing was 84.8 and 100% respectively, whereas those of ultrarapid PCR were 100 and 100%, respectively (Table II). These data revealed that ultrarapid PCR has superior sensitivity and specificity in clinical samples to direct sequencing, and parallels that of the PCR-Invader method, which is one of the commonly used PCR-based methodologies in current clinical practice.

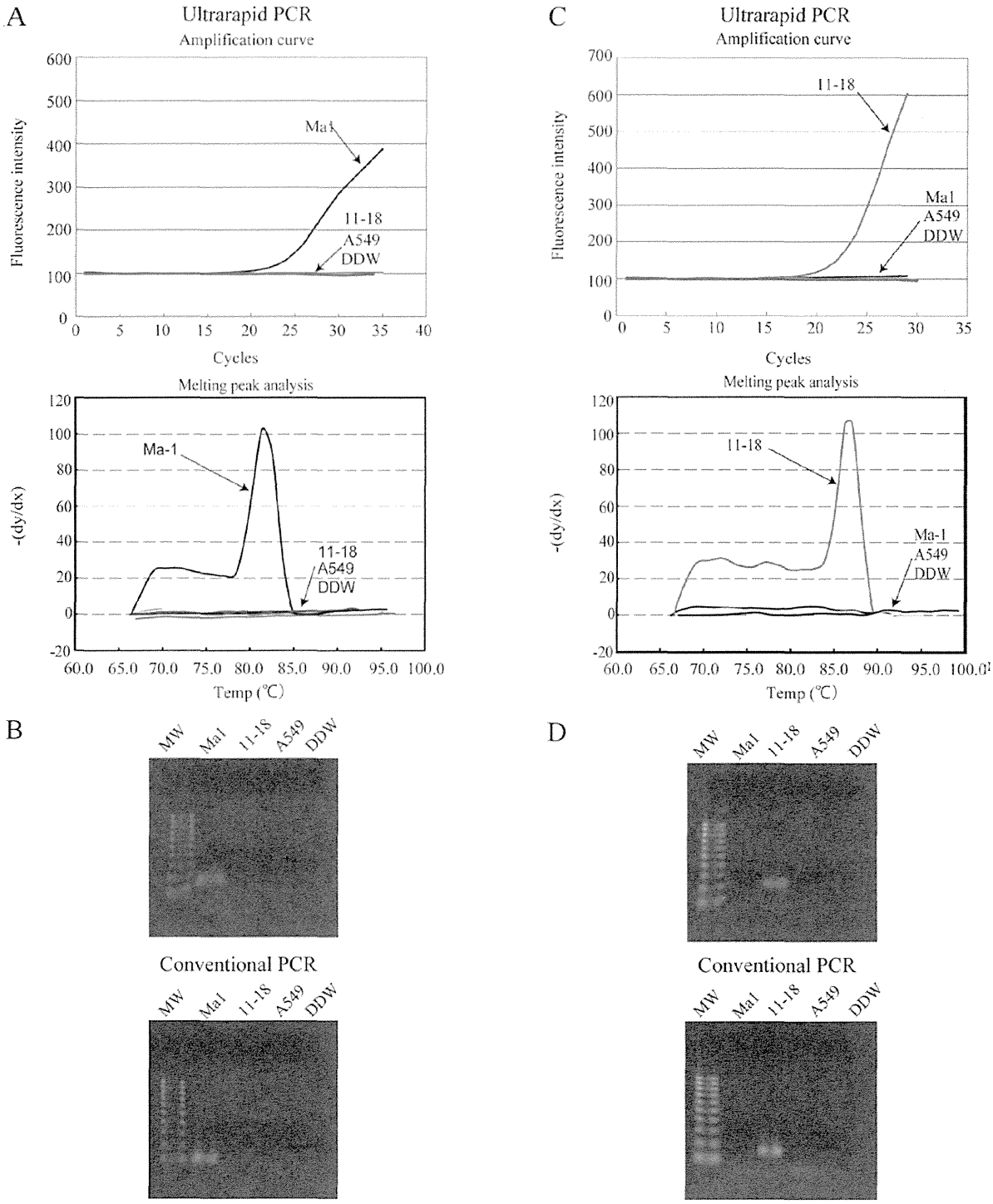


Figure 3. Specificity of the mutation-specific primers for the two most frequent *EGFR* mutations. (A) The delE746-A750-specific primers were tested on Ma1 cells harboring delE746-A750, 11-18 cells harboring L858R, A549 cells with the wild-type *EGFR*, and a negative control [double-distilled water, (DDW)] using ultrarapid PCR. The amplification and melting curve, and electrophoresed amplified product is shown. MW, 100 bp-DNA ladder. (B) The experiment was also performed using conventional PCR, and the results of electrophoresis of the corresponding products are shown. (C) The L858R-specific primers were tested on each cells and negative control using ultrarapid PCR. (D) The L858R-specific primers were tested on the same samples using conventional PCR, and the results of electrophoresis of the products are shown. EGFR, epidermal growth factor receptor.

*Ultrarapid detection of EGFR mutation in a patient with adenocarcinoma.* A 39-year-old woman with no history of smoking was referred to our hospital due to the presence of an abnormal shadow in her left upper lung field that was noticed during her regular medical checkup (Fig. 6A, upper panel). A computed tomography (CT) scan of the chest of this patient revealed a spiculated nodular shadow with a 35-mm diameter in the superior division of the left upper

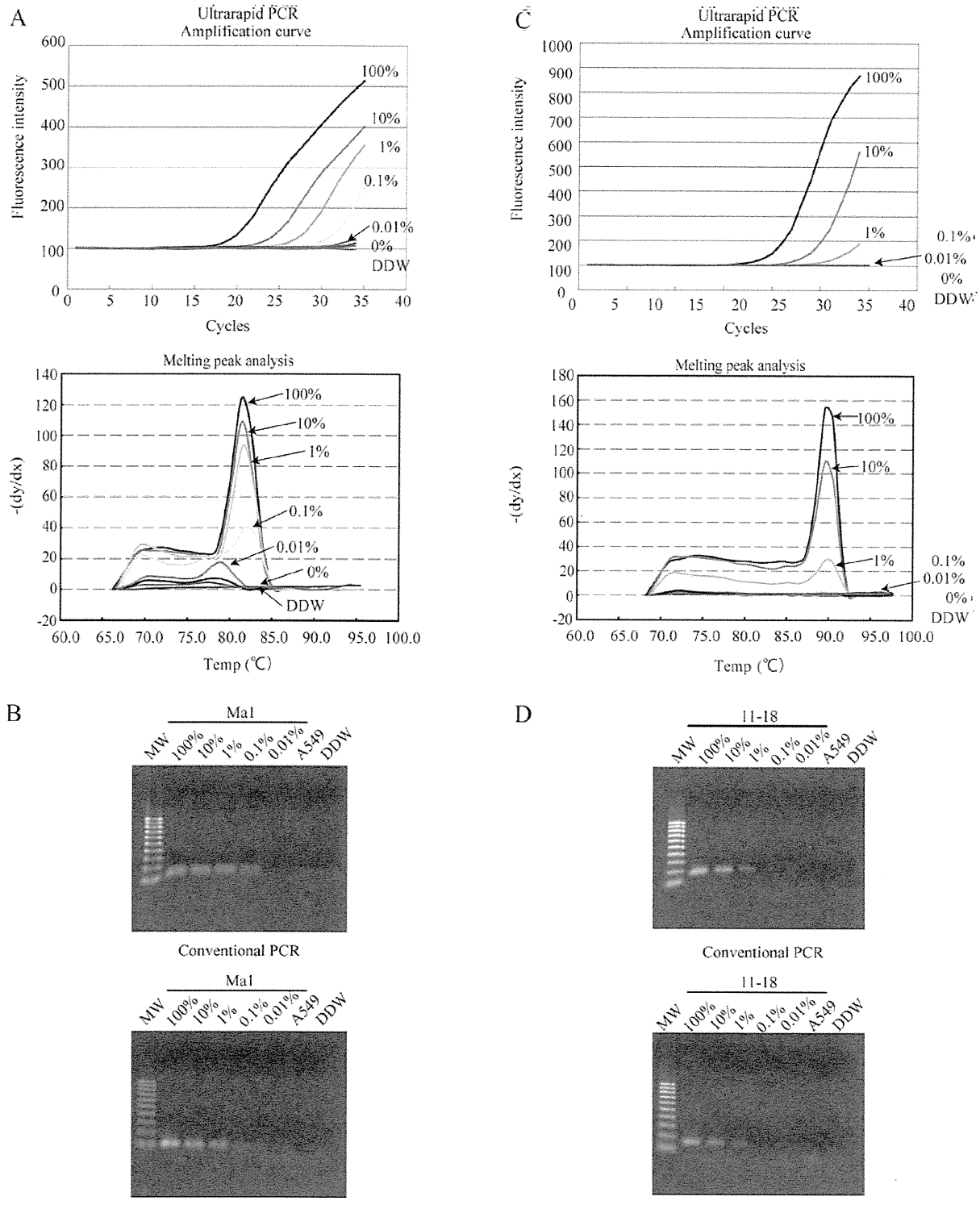


Figure 4. Sensitivity of mutation-specific ultrarapid PCR. (A) Ultrarapid PCR amplification of the delE746-A750 allele from a mixture of cell samples containing 100, 10, 1, 0.1, 0.01 and 0% of Ma1 cells harboring the mutation. As few as 0.1% of tumor cells with the delE746-A750 mutation could be detected. DDW, double-distilled water. (B) Conventional PCR amplification of the same samples as in A. Electrophoresis of the products showed the same detection limit as ultrarapid PCR. (C) Ultrarapid PCR amplification of the L858R allele from a mixture of cell samples containing 100, 10, 1, 0.1, 0.01 and 0% of 11-18 cells harboring the mutation. As few as 1% of tumor cells with the L858R mutation could be detected. (D) Conventional PCR amplification of the same samples as in C; electrophoresed products are shown. The same detection limit as with ultrarapid PCR was observed.

lobe (Fig. 6A, lower panel). F-2-deoxy-2-fluoro-D-glucose (FDG)-positron emission tomography revealed multiple lesions with high uptake in her liver and vertebrae. Based on the suspicion of adenocarcinoma with multiple metastases, we

Table I. Samples showing discordant results between sequencing and PCR detection methods.

| Case | Direct sequence | Conventional PCR | Ultrarapid PCR | PCR-Invader method |
|---|---|---|---|---|
| 1 | Wild-type | DelE746-A750 | DelE746-A750 | DelE746-A750 |
| 2 | Wild-type | DelE746-A750 | DelE746-A750 | DelE746-A750 |
| 3 | Wild-type | L858R | L858R | L858R |
| 4 | Wild-type | L858R | L858R | L858R |
| 5 | Wild-type | L858R | L858R | L858R |

Table II. Sensitivity and specificity of direct sequencing and mutation-specific ultrarapid PCR.

| | Direct sequence | Ultrarapid PCR |
|---|---|---|
| Sensitivity | 84.8% (28/33) | 100% (33/33) |
| Specificity | 100% (110/110) | 100% (110/110) |

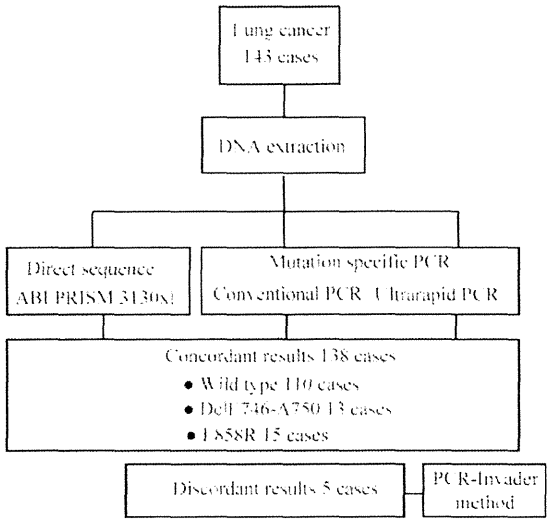


Figure 5. Detection of two major *EGFR* mutations in lung cancer samples. Tumor samples obtained during resection were tested for the presence of two major *EGFR* mutations using mutation-specific primers in ultrarapid PCR or conventional PCR. Direct sequencing was used as comparison, and PCR-Invader was used as a reflex test for samples with discordant results. EGFR, epidermal growth factor receptor.

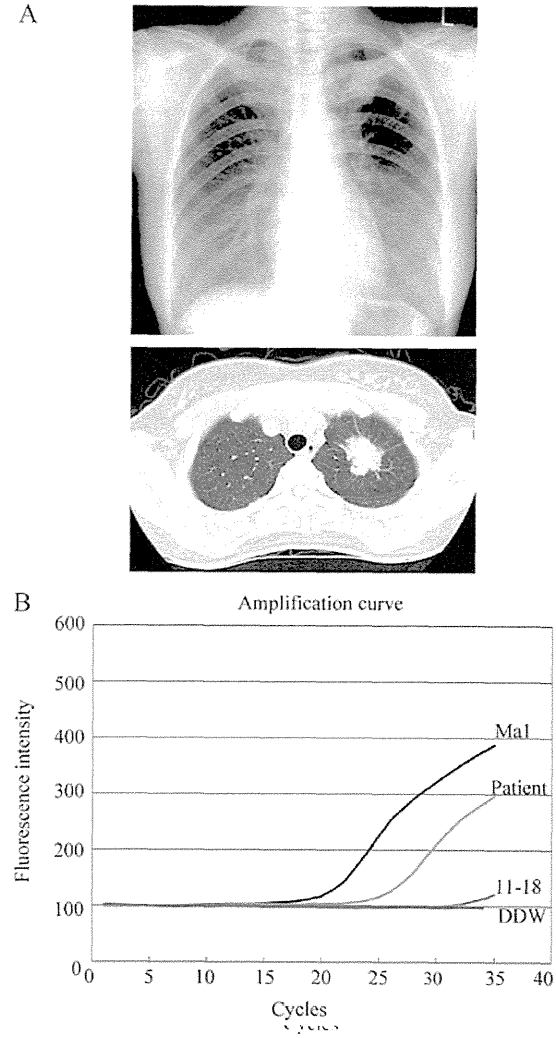


Figure 6. Mutation detection on a cytology sample obtained from a lung cancer patient by bronchoscopic examination. (A) Chest X-ray and computed tomography scan of the chest of a patient referred to our hospital on suspicion of lung cancer. (B) Results of mutation-specific ultrarapid PCR on a lavage sample collected by bronchoscopic examination. The presence of the delE746-A750 mutation was detected by ultrarapid PCR in <50 min after bronchoscopic examination.

preformed flexible bronchoscopic examination with washing, brushing and forceps biopsy. In addition to the cytological and histological examination of the lavage and biopsy specimens, we applied ultrarapid PCR analysis to the lavage sample. The lavage was centrifuged and DNA was extracted within 40 min after sample collection. Ultrarapid PCR analysis subsequently revealed the presence of the delE746-A750 *EGFR* mutation in her lavage sample, within 6 min (Fig. 6B). After waiting for confirmation of positive results by cytology and histology, which were obtained 3-4 days after bronchoscopic examination, the patient was diagnosed as having adenocarcinoma with an *EGFR* mutation (cT2aN0M1b, stage IV). She commenced treatment with 150 mg erlotinib/day immediately, and her lung CT scan at 6 weeks after the initiation of treatment revealed a marked improvement.

## Discussion

In the present study, we newly developed an ultrarapid PCR approach for detecting *EGFR* mutations. This method showed excellent specificity and sensitivity for clinical samples, which is superior to direct sequencing and is comparable to other PCR-based methodologies that are frequently used in modern laboratory practice. In addition, to our knowledge, this method has superior rapidity among the methodologies reported for *EGFR* mutation detection. Therefore, introduction of this technology to clinical practice may open new opportunities for diagnosis and therapy of lung cancer patients.

In the present study, we used direct sequencing as a method against which to compare our newly developed ultrarapid mutation-specific PCR, since it is the historical standard and many studies reporting novel methodology have used it for comparison (28). However, even when using macrodissection to enrich tumor DNA in a sample, the sensitivity of direct sequencing was 84.8%, whereas that of ultrarapid PCR was 100%. In addition, it is noteworthy that the mutation analysis results of the five sequencing-discordant samples were consistent between ultrarapid PCR and PCR-Invader, one of the current laboratory-standard PCR-based assays. In a recent study, these frequently used PCR-based assays, i.e., PCR-Invader, PNA-LNA PCR clamp, Scorpion ARMS and cycleave PCR, could detect mutations in at least 1% of mutant/wild-type allele-admixture samples, and showed equal sensitivity and specificity in clinical specimens (tissue and cytology samples) (29). Based on the detection limit in the admixture analysis and the results of surgical resected tissues in our study, the ultrarapid PCR we present here appears to be comparable to current sensitive laboratory-standard PCR-based methodologies for detecting *EGFR* mutations.

Moreover, compared to the other current PCR-based methods, ultrarapid PCR has several advantages. The first significant advantage is the rapid turnaround time for amplification and detection (<10 min in the experiments reported here). This machine employed a novel thermo-control mechanism, with a thermal ramp rate of up to 20˚C/sec; this is the shortest ramp rate among the published ramp rate for thermal cyclers (30). By combining this machine with our newly designed mutation-specific primers, choosing an adequate polymerase, optimizing the composition of the reaction mixture, and adjusting the thermal conditions, we have here developed the fastest real-time detection system for *EGFR* mutation screening to date.

The second advantage of our approach is its simplicity and cost-effectiveness. We used the double-strand DNA-binding dye, SYBR-Green I, for real-time detection of the PCR product, whereas other systems use fluorogenic probes. Since *EGFR* mutation detection is a fundamentally qualitative detection, we believe the simplicity, flexibility, and cost-effectiveness of detection using SYBR-Green I may be sufficient for the purpose. Besides their relative expense, the use of fluorogenic probes complicates modification and optimization of real-time PCR, and primers/probes need to be designed according to specific rules, due to the simultaneous annealing of the primers and probes in real-time PCR (31).

Our system was designed to detect the two major *EGFR* mutations for which the majority of clinical evidence supports the use of EGFR TKIs; it is not able to detect all *EGFR* mutations, similar to other PCR-based systems. However, clinical data supporting the use of EGFR TKIs for less common mutations are emerging, and adaptation of the detection system to these more rare mutations will be required in the near feature. Our system may present a convenient way to do this, since it would only require the design of new primers and adjustment of the PCR conditions.

Our ultrarapid mutation-specific PCR will open new potential applications for the clinical management of lung cancer patients. The representative case we presented in the present study illustrates three important characteristics of this test. First, this test can be applied to cytology samples obtained in routine clinical practice, such as bronchoscopic lavage. Second, since the test result can be obtained within <50 min after sample collection, treatment with TKIs can be started very rapidly. Third, since this system is simple and less expensive, this test may enable clinicians to request repeat tests for *EGFR* mutation for a given patient. Repeated testing for *EGFR* mutations is in demand, particularly for recurrent or metastatic lesions, to allow selection of optimal treatment. Eventually, this test can be used as a point-of-care approach, which has not been available for *EGFR* testing to date.

In conclusion, we developed a simple, rapid, and less expensive *EGFR* mutation detection system. This system has comparable sensitivity and specificity to that of recently developed laboratory-standardized PCR-based methods, and, unlike these methods, offers high speed performance. Given the simplicity of the methodology, this system may help to usher in a new phase in *EGFR* mutation testing for the diagnosis and treatment of lung cancer patients.

## References

1. Ferlay J, Parkin DM and Steliarova-Foucher E: Estimates of cancer incidence and mortality in Europe in 2008. Eur J Cancer 46: 765-781, 2010.
2. Azzoli CG, Baker S Jr, Temin S, *et al*: American Society of Clinical Oncology Clinical Practice Guideline update on chemotherapy for stage IV non-small-cell lung cancer. J Clin Oncol 27: 6251-6266, 2009.
3. Lynch TJ, Bell DW, Sordella R, *et al*: Activating mutations in the epidermal growth factor receptor underlying responsiveness of non-small-cell lung cancer to gefitinib. N Engl J Med 350: 2129-2139, 2004.
4. Maemondo M, Inoue A, Kobayashi K, *et al*: Gefitinib or chemotherapy for non-small-cell lung cancer with mutated EGFR. N Engl J Med 362: 2380-2388, 2010.
5. Mitsudomi T, Morita S, Yatabe Y, *et al*: Gefitinib versus cisplatin plus docetaxel in patients with non-small-cell lung cancer harbouring mutations of the epidermal growth factor receptor (WJTOG3405): an open label, randomised phase 3 trial. Lancet Oncol 11: 121-128, 2010.
6. Mok TS, Wu YL, Thongprasert S, *et al*: Gefitinib or carboplatin-paclitaxel in pulmonary adenocarcinoma. N Engl J Med 361: 947-957, 2009.
7. Rosell R, Carcereny E, Gervais R, *et al*: Erlotinib versus standard chemotherapy as first-line treatment for European patients with advanced EGFR mutation-positive non-small-cell lung cancer (EURTAC): a multicentre, open-label, randomised phase 3 trial. Lancet Oncol 13: 239-246, 2012.
8. Zhou C, Wu YL, Chen G, *et al*: Erlotinib versus chemotherapy as first-line treatment for patients with advanced EGFR mutation-positive non-small-cell lung cancer (OPTIMAL, CTONG-0802): a multicentre, open-label, randomised, phase 3 study. Lancet Oncol 12: 735-742, 2011.

9. Han JY, Park K, Kim SW, *et al*: First-SIGNAL: first-line single-agent iressa versus gemcitabine and cisplatin trial in never-smokers with adenocarcinoma of the lung. J Clin Oncol 30: 1122-1128, 2012.
10. Paez JG, Janne PA, Lee JC, *et al*: EGFR mutations in lung cancer: correlation with clinical response to gefitinib therapy. Science 304: 1497-1500, 2004.
11. Pao W, Miller V, Zakowski M, *et al*: EGF receptor gene mutations are common in lung cancers from 'never smokers' and are associated with sensitivity of tumors to gefitinib and erlotinib. Proc Natl Acad Sci USA 101: 13306-13311, 2004.
12. Shigematsu H, Lin L, Takahashi T, *et al*: Clinical and biological features associated with epidermal growth factor receptor gene mutations in lung cancers. J Natl Cancer Inst 97: 339-346, 2005.
13. Han SW, Kim TY, Hwang PG, *et al*: Predictive and prognostic impact of epidermal growth factor receptor mutation in non-small-cell lung cancer patients treated with gefitinib. J Clin Oncol 23: 2493-2501, 2005.
14. Kosaka T, Yatabe Y, Endoh H, Kuwano H, Takahashi T and Mitsudomi T: Mutations of the epidermal growth factor receptor gene in lung cancer: biological and clinical implications. Cancer Res 64: 8919-8923, 2004.
15. Pao W and Ladanyi M: Epidermal growth factor receptor mutation testing in lung cancer: searching for the ideal method. Clin Cancer Res 13: 4954-4955, 2007.
16. Mitsudomi T and Yatabe Y: Mutations of the epidermal growth factor receptor gene and related genes as determinants of epidermal growth factor receptor tyrosine kinase inhibitors sensitivity in lung cancer. Cancer Sci 98: 1817-1824, 2007.
17. Hall JG, Eis PS, Law SM, *et al*: Sensitive detection of DNA polymorphisms by the serial invasive signal amplification reaction. Proc Natl Acad Sci USA 97: 8272-8277, 2000.
18. Naoki K, Soejima K, Okamoto H, *et al*: The PCR-invader method (structure-specific 5' nuclease-based method), a sensitive method for detecting EGFR gene mutations in lung cancer specimens; comparison with direct sequencing. Int J Clin Oncol 16: 335-344, 2011.
19. Nagai Y, Miyazawa H, Huqun, *et al*: Genetic heterogeneity of the epidermal growth factor receptor in non-small cell lung cancer cell lines revealed by a rapid and sensitive detection system, the peptide nucleic acid-locked nucleic acid PCR clamp. Cancer Res 65: 7276-7282, 2005.
20. Yatabe Y, Hida T, Horio Y, Kosaka T, Takahashi T and Mitsudomi T: A rapid, sensitive assay to detect EGFR mutation in small biopsy specimens from lung cancer. J Mol Diagn 8: 335-341, 2006.
21. Kimura H, Kasahara K, Kawaishi M, *et al*: Detection of epidermal growth factor receptor mutations in serum as a predictor of the response to gefitinib in patients with non-small-cell lung cancer. Clin Cancer Res 12: 3915-3921, 2006.
22. Takata M, Chikumi H, Miyake N, *et al*: Lack of AKT activation in lung cancer cells with EGFR mutation is a novel marker of cetuximab sensitivity. Cancer Biol Ther 13: 369-378, 2012.
23. Fujimoto T, Konagaya M, Enomoto M, *et al*: Novel high-speed real-time PCR method (Hyper-PCR): results from its application to adenovirus diagnosis. Jpn J Infect Dis 63: 31-35, 2010.
24. Barbau-Piednoir E, Botteldoorn N, Yde M, Mahillon J and Roosens NH: Development and validation of qualitative SYBR®Green real-time PCR for detection and discrimination of *Listeria* spp. and *Listeria monocytogenes*. Appl Microbiol Biotechnol 97: 4021-4037, 2013.
25. Bustin SA: Absolute quantification of mRNA using real-time reverse transcription polymerase chain reaction assays. J Mol Endocrinol 25: 169-193, 2000.
26. Newton CR, Graham A, Heptinstall LE, *et al*: Analysis of any point mutation in DNA. The amplification refractory mutation system (ARMS). Nucleic Acids Res 17: 2503-2516, 1989.
27. Newton CR, Kalsheker N, Graham A, *et al*: Diagnosis of $\alpha_1$-antitrypsin deficiency by enzymatic amplification of human genomic DNA and direct sequencing of polymerase chain reaction products. Nucleic Acids Res 16: 8233-8243, 1988.
28. Ellison G, Zhu G, Moulis A, Dearden S, Speake G and McCormack R: EGFR mutation testing in lung cancer: a review of available methods and their use for analysis of tumour tissue and cytology samples. J Clin Pathol 66: 79-89, 2013.
29. Goto K, Satouchi M, Ishii G, *et al*: An evaluation study of EGFR mutation tests utilized for non-small-cell lung cancer in the diagnostic setting. Ann Oncol 23: 2914-2919, 2012.
30. Kim YH, Yang I, Bae YS and Park SR: Performance evaluation of thermal cyclers for PCR in a rapid cycling condition. Biotechniques 44: 495-496, 498, 500 passim, 2008.
31. Nitsche A: Oligonucleotide design for in-house real-time PCR applications in microbiology. In: Real-Time PCR in Microbiology. Mackay IM (ed). Caister Academic Press, Norfolk, pp41-69, 2007.

# Favorable effect of the combination of vinorelbine and dihydropyrimidine dehydrogenase-inhibitory fluoropyrimidine in *EGFR*-mutated lung adenocarcinoma: Retrospective and *in vitro* studies

HIROKI IZUMI[1], HIROKAZU TOUGE[1], TADASHI IGISHI[1], HARUHIKO MAKINO[1], SHIZUKA NISHII-ITO[1], MIYAKO TAKATA[1], HIROFUMI NAKAZAKI[1], YASUTO UEDA[1], SHINGO MATSUMOTO[1], MASAHIRO KODANI[1], JUN KURAI[1], KENICHI TAKEDA[1], TOMOHIRO SAKAMOTO[1], MASAAKI YANAI[1], NATSUMI TANAKA[1], CHAITANYA S. NIRODI[2] and EIJI SHIMIZU[1]

[1]Division of Medical Oncology and Molecular Respirology, Faculty of Medicine, Tottori University, Yonago, Tottori 683-8504, Japan; [2]Department of Oncologic Sciences, Mitchell Cancer Institute, University of South Alabama, Mobile, AL 36604, USA

Received October 10, 2014; Accepted November 25, 2014

DOI: 10.3892/ijo.2015.2815

**Abstract.** Although cytotoxic chemotherapy is essential in epidermal growth factor receptor (*EGFR*)-mutated non-small cell lung cancer (NSCLC), it is unclear which regimen is most effective. We retrospectively compared the efficacy of standard platinum-based chemotherapy with that of combination chemotherapy using vinorelbine (VNR) plus dihydropyrimidine dehydrogenase-inhibitory fluoropyrimidine (DIF) in *EGFR*-mutated lung adenocarcinomas, and we investigated a potential mechanism by which the combination chemotherapy of VNR + DIF was favorable in the treatment of *EGFR*-mutated lung adenocarcinoma *in vitro*. In our retrospective analysis, the response rate and disease control rate afforded by the VNR + DIF treatment tended to be better than those by platinum-based chemotherapy, and the progression-free survival of the 24 VNR + DIF-treated patients was significantly longer than that of the 15 platinum-based chemotherapy patients. In *EGFR*-mutated PC9 cells, VNR induced EGFR dephosphorylation at a clinically achievable concentration. 1BR3-LR cells, a line of fibroblast cells transfected with a mutant *EGFR* construct, were completely resistant to gefitinib in the medium containing 10% fetal bovine serum (FBS), whereas the sensitivity of these cells to gefitinib was increased in 0.5% FBS-containing medium. Similarly, the sensitivity of 1BR3-LR cells to VNR was increased when they were cultured in low-serum condition. In addition, sodium orthovanadate ($Na_3VO_4$) inhibited the EGFR dephosphorylation induced by VNR or gefitinib and suppressed the cell growth inhibition by these agents in PC9 cells. VNR and gefitinib showed synergistic cell growth inhibition in combination with 5-fluorouracil (5-FU) in PC9 cells. We propose that the EGFR dephosphorylation induced by VNR is related to cell growth inhibitory activity of VNR, and that this is one of the mechanisms of the synergistic effect of VNR + 5-FU in *EGFR*-mutated lung cancer cells. In conclusion, the combination chemotherapy of VNR + DIF may be a promising treatment for NSCLC patients with *EGFR* mutations.

*Correspondence to:* Dr Tadashi Igishi, Division of Medical Oncology and Molecular Respirology, Faculty of Medicine, Tottori University, 36-1 Nishi-machi, Yonago 683-8504, Japan
E-mail: igishi@med.tottori-u.ac.jp

*Key words:* vinorelbine, dihydropyrimidine dehydrogenase-inhibitory fluoropyrimidine, 5-fluorouracil, epidermal growth factor receptor, lung adenocarcinoma

## Introduction

Lung cancer is the leading cause of cancer-related death worldwide. More than 80% of lung cancers are non-small cell lung cancers (NSCLCs), and lung adenocarcinoma is the most common type of NSCLC. The median survival of patients with metastatic NSCLC treated with cytotoxic chemotherapy agents is 10-12 months (1,2).

Epidermal growth factor receptor (EGFR), a member of the family of growth factor receptor tyrosine kinases, is expressed in a variety of solid cancers. *EGFR* somatic mutations were identified in 5-40% of NSCLCs, and is especially common in never-smokers, women, Asians, and patients with adenocarcinoma (3-6). NSCLCs harboring-activated *EGFR* mutations are addicted to EGFR signaling, and treatment with small-molecule EGFR-tyrosine kinase inhibitors (TKIs) such as gefitinib and erlotinib demonstrated dramatic responses to lung adenocarcinomas with *EGFR* mutations (7,8). However, almost all lung adenocarcinoma patients with *EGFR* mutations

who respond to EGFR-TKIs ultimately develop resistance to these agents. Therefore, to prolong the survival time of advanced NSCLC patients with *EGFR* mutations, conventional cytotoxic chemotherapy is necessary regardless of whether it is administered before or after treatment with EGFR-TKIs.

At present, the combination of platinum with one of several chemotherapeutic agents [docetaxel, paclitaxel, gemcitabine, vinorelbine (VNR), irinotecan, pemetrexed or FT-5-chloro-2,4-dihydroxypyridine-potassium oxonate (S-1)] is considered a standard chemotherapy for advanced NSCLC (1,2,9,10). However, non-platinum combinations of third-generation drugs such as gemcitabine + VNR have less toxicity and almost equivalent efficacy compared to platinum-based chemotherapy (11). Therefore, non-platinum combination chemotherapy can be an option as a first-line treatment, even in patients with advanced NSCLC harboring *EGFR* mutations.

VNR, which is widely used to treat solid tumors such as NSCLC and breast cancer, is a semisynthetic vinca-alkaloid derived from vinblastine. This chemotherapeutic agent is one of the standard treatment agents for elderly patients with NSCLC (12), and, in combination with cisplatin, VNR is the only third-generation drug that demonstrated a consistent improvement of survival in the adjuvant setting of resected NSCLC (13-15).

UFT is an oral anticancer agent combining tegafur (FT) and uracil at a molar ratio of 1:4. FT is a prodrug of 5-fluorouracil (5-FU), and uracil is a competitive and reversible inhibitor of dihydropyrimidine dehydrogenase (DPD), the rate-limiting enzyme responsible for the catabolism of 5-FU. S-1 is a novel oral fluorouracil antitumor drug that combines FT, 5-chloro-2,4-dihydroxypyridine (which inhibits DPD activity), and potassium oxonate (which reduces gastrointestinal toxicity). UFT and S-1 are referred to as dehydrogenase-inhibitory fluoropyrimidine (DIF).

UFT is effective in prolonging the survival of patients with NSCLC after surgical resection (16,17). In a recent phase III trial, the combination chemotherapy of S-1 with carboplatin was not inferior in terms of overall survival (OS) compared with a standard chemotherapy, carboplatin and paclitaxel, for patients with advanced NSCLC (9). These results suggest the potential of DIF as a chemotherapeutic agent for advanced NSCLC.

We reported the schedule-dependent synergistic effect of VNR and subsequent 5-FU or UFT on NSCLC *in vitro* and in an animal model (18). Based on these preclinical data, we conducted two phase II studies of VNR + DIF, under which VNR was infused on days 1 and 8, and 600 mg/day UFT or 80 mg/m$^2$/day S-1 was administered daily from day 2 to 6 and from day 9 to 13 in a 3-week cycle. The combination therapy of VNR + UFT was shown to be feasible and active in the treatment of elderly patients with advanced NSCLC (19). Promising results were also observed in unselected advanced NSCLC patients treated with the combination of VNR + S-1 (20).

In the process of clinical trials and clinical practice applying the combination treatment of VNR + DIF for advanced NSCLC, we noticed that patients exhibiting long-term stable disease tended to harbor *EGFR* mutations. This finding raised a hypothesis that the combination treatment of VNR + DIF may be specifically effective in NSCLC patients with *EGFR* mutations.

In the present study, we retrospectively compared the efficacy of the combination treatment of VNR + DIF with that of the standard platinum-based chemotherapy in patients with lung adenocarcinoma harboring *EGFR* mutations. We also sought to identify the mechanism by which the combination chemotherapy of VNR + DIF was more favorable than platinum-based chemotherapy in NSCLC harboring *EGFR* mutations *in vitro*.

## Materials and methods

*Comparison of the effects of chemotherapies.* We retrospectively reviewed 39 lung adenocarcinoma patients harboring *EGFR* mutations who were diagnosed from November, 2004 to March, 2013 at Tottori University Hospital in Yonago, Japan and who received the combination therapy of VNR + DIF or platinum-based chemotherapy for the first cytotoxic chemotherapy. The presence of *EGFR* mutation was evaluated by the polymerase chain reaction (PCR)-invader method (BML, Inc., Tokyo, Japan). *EGFR* mutation analyses were not performed in four cases. These patients achieved long-term progression-free survival (PFS) times of >6 months with gefitinib treatment. The PFS was <6 months in >95% of the *EGFR* mutation-negative patients (21). Thus, we considered these four patients as *EGFR* mutation-positive cases.

The differences between the two groups were compared by the Mann-Whitney test and $\chi^2$ or Fisher's exact test for numerical and categorized data, respectively. Tumor response was evaluated according to the Response Evaluation Criteria in Solid Tumors (RECIST) (22). The OS and PFS times following the first-line cytotoxic chemotherapy was assessed using the Kaplan-Meier method and compared by the log-rank test. $P<0.05$ was considered significant.

*Chemicals and reagents.* VNR (Kyowa Hakko Kirin Co., Ltd., Tokyo, Japan) was dissolved in distilled water and stored at -20˚C. A stock solution of cisplatin (CDDP) (Nippon Kayaku Co., Ltd., Tokyo, Japan) was reconstituted with water, diluted in 0.9% sodium chloride solution, and stored at -20˚C. Gefitinib (AstraZeneca, Cheshire, UK) and 5-FU (Kyowa Hakko Kirin Co., Ltd.) were dissolved in dimethyl sulfoxide and stored at -20˚C. 3-(4,5-Dimethylhiazol-2-yl)-2,5-diphenyltetrazolium bromide (MTT) (Wako Pure Chemical Industries, Ltd., Osaka, Japan) was dissolved in phosphate-buffered saline (PBS) and stored at -20˚C.

*Cell lines and cultures.* The human NSCLC cell line PC9, which harbors an *EGFR* exon 19 deletion mutation (ΔE746-A750) (23) was obtained from the RIKEN BioResource Center (Ibaraki, Japan). The fibroblast cell line 1BR3, stably transfected with a mutant *EGFR* construct with an L858R replacement in exon 21 (1BR3-LR), was a generous gift from Dr David J. Chen (24). The PC9 cells were maintained in RPMI-1640 medium supplemented with 10% fetal bovine serum (FBS) and antibiotics (100 U/ml penicillin and 100 μg/ml streptomycin). 1BR3-LR cells were maintained in MEM-α medium supplemented with 10% FBS and antibiotics (100 U/ml penicillin, 100 μg/ml streptomycin, and 2 μg/ml